Summer 1990

Plio-Pleistocene Stratigraphy and Tectonic Evolution of the Northern Ohara Depression-Wakarara Range, North Island, New Zealand

Craig Fraser Erdman
Western Washington University

PLIO-PLEISTOCENE STRATIGRAPHY AND TECTONIC EVOLUTION OF THE NORTHERN OHARA DEPRESSION-WAKARARA RANGE, NORTH ISLAND, NEW ZEALAND

by

Craig Fraser Erdman

accepted in partial completion of the requirements for the degree of Master of Science

Dean of Graduate School

Advisory Committee

Chairman

MASTER'S THESIS

In presenting this thesis in partial fulfillment of the requirements for a master's degree at Western Washington University, I agree that the Library shall make its copies freely available for inspection. I further agree that extensive copying of this thesis is allowable only for scholarly purposes. It is understood, however, that any copying or publications of this thesis for commercial purposes, or for financial gain, shall not be allowed without my written permission.

Signature ________________

Date August 3, 1990

MASTER'S THESIS

In presenting this thesis in partial fulfillment of the requirements for a master's degree at Western Washington University, I grant to Western Washington University the non-exclusive royalty-free right to archive, reproduce, distribute, and display the thesis in any and all forms, including electronic format, via any digital library mechanisms maintained by WWU.

I represent and warrant this is my original work and does not infringe or violate any rights of others. I warrant that I have obtained written permissions from the owner of any third party copyrighted material included in these files.

I acknowledge that I retain ownership rights to the copyright of this work, including but not limited to the right to use all or part of this work in future works, such as articles or books.

Library users are granted permission for individual, research and non-commercial reproduction of this work for educational purposes only. Any further digital posting of this document requires specific permission from the author.

Any copying or publication of this thesis for commercial purposes, or for financial gain, is not allowed without my written permission.

Name: Craig F. Erdman

Signature: ____________________

Date: May 15, 2018

PLIO-PLEISTOCENE STRATIGRAPHY AND TECTONIC EVOLUTION OF THE NORTHERN OHARA DEPRESSION-WAKARARA RANGE, NORTH ISLAND, NEW ZEALAND

A thesis presented to the faculty
of Western Washington University

in partial fulfillment
of the requirements for the degree of
Master of Science

by

Craig F. Erdman
August, 1990

ABSTRACT

Development of the Ohara Depression and uplift of the Ruahine and Wakarara Ranges followed an increase of the convergence rate between the Pacific and Australian plates. The Ohara Depression is a trough of Plio-Pleistocene sediments that crops out between the Ruahine and Wakarara Ranges. Two episodes of uplift during the late Pliocene and Pleistocene are recorded in the geologic record. Initial uplift occurred in the late Pliocene followed by subsidence through the early Pleistocene. The greatest uplift occurred during the mid-Pleistocene, and is recorded by deposition of a 200-250 m-thick conglomerate unit. Although compressional structures are present within and to the east of the Ohara Depression, there is a partitioning of strain between the eastern front of the Wakarara Range and the Ohara Depression. Coast-perpendicular shortening dominates along the eastern Wakarara Range front and translation accompanied by coast-parallel shortening occurs within the Ohara Depression and along the Ruahine and Mohaka faults. Within the northern Ohara Depression, the Big Hill fault transfers motion from the Ruahine fault to the Mohaka fault. The Mohaka fault serves as a boundary between the two strain domains, shielding the part of the Ohara Depression west of the Wakarara Range from contraction.

ACKNOWLEDGEMENTS

As I sit here with only a few hours left (which is pretty typical, but I **am** getting better) to hand in this document to the Dean, my mind blurs as I sleepily try to think of all the people that have helped me on the way to completing this thesis. Around the department, none of us could get through without harassing Patty and Vicki with the same questions they hear every year, if not every quarter. Thanks, you two, for your patience, if only on the surface!

I also thank Dave Engebretson who gave me a lot of support that first year. We were both going through our personal hells. I really appreciated your classes and you as a person. I wish you the best.

None of this would have been possible without the Kelsey-Cashman clan. Thanks, Sue, for the time spent in the field and, after two years, the help and support in the last stages of completing my thesis. Harvey, of course, has been a neotectono-geohydrodynamo when it came down to the last six months and cranking out four graduate students. I really appreciate the time and energy you put into your editorial comments. Thanks for the trip to down-under, though I know it lasted a good deal longer than any of us expected!

I also thank the New Zealand farmers in my field area, especially Bill Glazebrook, Harvey Boyden, Dick Timpany, and Trevor Smythe. They were all very friendly, open people. I also can't forget Doug and Sue Callendar for the fishing expedition at Tongariro Prison Farm, nor Taffy Metcalfe, who was quite a character.

From the New Zealand Geological Survey, I give a lot of thanks and gratitude to Huntly Cutten for his mapping of the Big Hill fault and the area along the Ngaruroro River, for fishing companionship and putting me up (putting up with me?) at his house. Thanks also to Kelvin Berryman who helped with a lot of the initial logistics of getting this project going. Alan Beu looked at many fossil samples I collected which have been extremely valuable for age-dating and determining environments of deposition. Thank you very much! I also thank George Scott who inspected microfossil samples.

I thank Brad Pillans and his students for analyzing tephra glass-chemistries by micro-probe.

I thank an anonymous group of people who heard me groan about this thesis for months until I finally finished! I never could have done it without your fellowship. Thanks also to Tim Redfield, Galan and Jacquie McInelly, Jennie De Chant, Terri Plake, Erik Hansen, Bruce Halibisky, my mother, Marjorie Erdman and the rest of my family and all those miffed people who I didn't name.

Lastly, as a geologist I never thought I'd say it and mean it, but: Thank you, God, this bloody thing is finished!

TABLE OF CONTENTS

LIST OF FIGURES

LIST OF TABLES

INTRODUCTION

New Zealand lies along the active Australia-Pacific plate boundary (Figure 1) (Le Pichon, 1968). Along the east coast of the North Island, the Pacific plate obliquely subducts beneath the Australian plate along the Hikurangi trench. The Pacific plate presently converges toward the North Island at a rate of approximately 44 mm/yr at the southern end of Hawke Bay (Figure 1) (using the finite rotation pole of Gordon et al., 1988). The rate of convergence has been operative since the 3.4 my BP change in the Antarctic-Pacific spreading rate (Harbert and Cox, 1989). Numerous features and structures characteristic of a forearc setting are active today along the Hikurangi margin; these include strike-slip faults, arcward-dipping thrust faults, a seaward-building subduction complex, trench-slope basins, accretionary highs and a frontal ridge (Figure 1) (Lewis, 1980; Berryman, 1984; Davey et al., 1986).

Oblique convergence results in strain partitioning across the forearc of the North Island. Lewis (1980) modified a model of Walcott (1978) to propose that compressional features will be found outboard, with a gradual transition into a strike-slip belt inboard. The inboard strike-slip zone corresponds with the faults in and adjacent to the Axial Ranges (Walcott, 1978) (Figure 1). From the Hikurangi Trench to the coast, folding of Neogene strata and thrusting along arcward steepening faults are evident in seismic

Figure 1) Location map of study area (box delineating Figures 2, 8, 9 and 13) in central Hawke's Bay showing the major tectonic features. Inset shows plate tectonic configuration and the present-day instantaneous velocity of the Pacific plate towards the Australian plate at the latitude of Hawke Bay. On inset: MWF, Mohaka-Wellington fault; AR, Axial Ranges; FB, forearc basin.

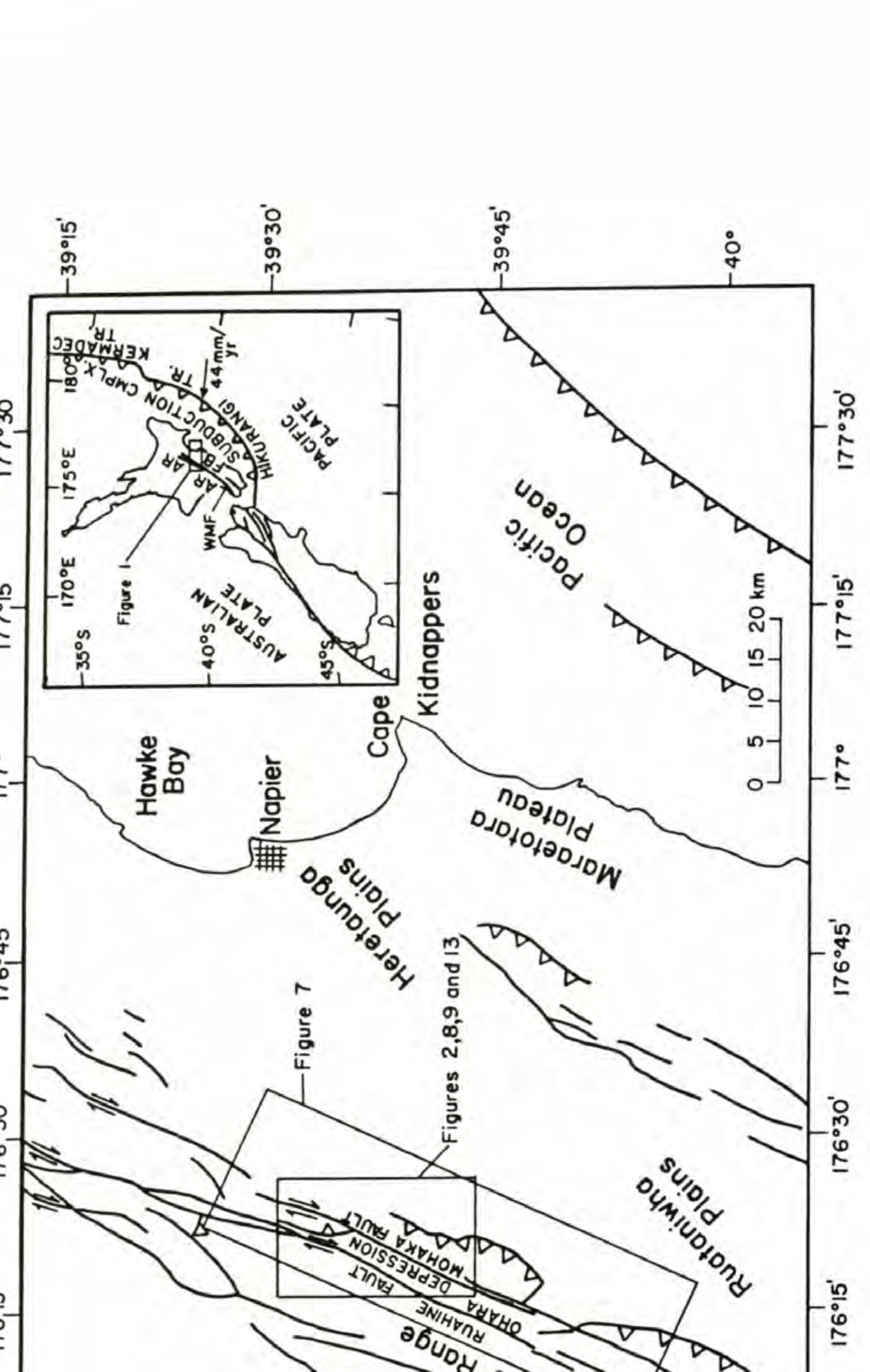

Hawke Bay
Napier
Cape Kidnappers
Heretaunga Plains
Maraetotara Plateau
Pacific Ocean
Ruataniwha Plains
Ruahine Range
RUAHINE FAULT
MOHAKA FAULT
DEPRESSION
OHARA
Figure 7
Figures 2,8,9 and 13
0 5 10 15 20 km
176°
176°15'
176°30'
176°45'
177°
177°15'
177°30'
39°15'
39°30'
39°45'
40°
AUSTRALIAN PLATE
PACIFIC PLATE
HIKURANGI SUBDUCTION CMPLX.
KERMADEC TR.
TR.
44 mm/yr
Figure 1
WMF
FB
AR
35°S
40°S
45°S
170°E
175°E
180°

profiles (Davey et al., 1986). In the southern Hawke's Bay region, recent studies of the faulting of Plio-Pleistocene sediments near the coast indicates extension is occurring in the Maraetotara Plateau (Figure 1) (Cashman and Kelsey, 1990). Between Hawke Bay and the Mohaka fault, Cutten et al. (1988) document a late Quaternary right lateral slip rate of 4.5 mm/yr on the Rangiora fault. Farther inboard, the present-day lateral slip rate on the Mohaka fault is 3.0-4.0 mm/yr (Hull, 1983; Hull, 1985; Raub, 1985) and is approximately 1-2 mm/yr on the Ruahine fault (Beanland and Berryman, 1987) (Figure 1).

The Ruahine Range forms the Axial Ranges of the central part of the North Island. The Range is bound on the east by the Ruahine fault (Figure 1). East of the Ruahine fault is the Mohaka fault. Between the Ruahine fault and the Mohaka fault, at the northern end of the Ruahine Range, lies the Ohara Depression (Kingma, 1958) (Figure 1). I mapped the northern Ohara Depression and the adjacent region along the eastern front of the central Axial Ranges (Figures 1 and 2) to better define the faulting and deformational styles in late Neogene sediments across a portion of the subaerially exposed forearc. Activity along the Mohaka and Ruahine faults over the past 2 million years has preserved a sequence (approx. 800 m) of Mangapanian (late Pliocene) to Nukumaruan (latest Pliocene to early Pleistocene) marine sediments within the northern part of the Ohara Depression.

Figure 2) Geologic map of the northern Ohara Depression and the Wakarara Range region. Mz, Torlesse Supergroup; Tpkm, Kaumatua Formation; Tpsb, Sentry Box Limestone; Tpmm, Mount Mary Limestone; TQoh, Ohara Mudstone; Qke, Kereru Limestone; Qok, Okauawa Formation; Qpu, Poutaki Pumiceous Formation; Qsg, Salisbury gravel lithofacies; HA, Herricks anticline; HS, Herricks syncline; TFF, Thorn Flat fault; BS, Balcony syncline; PF, Poporangi fault. See lithologic descriptions in text.

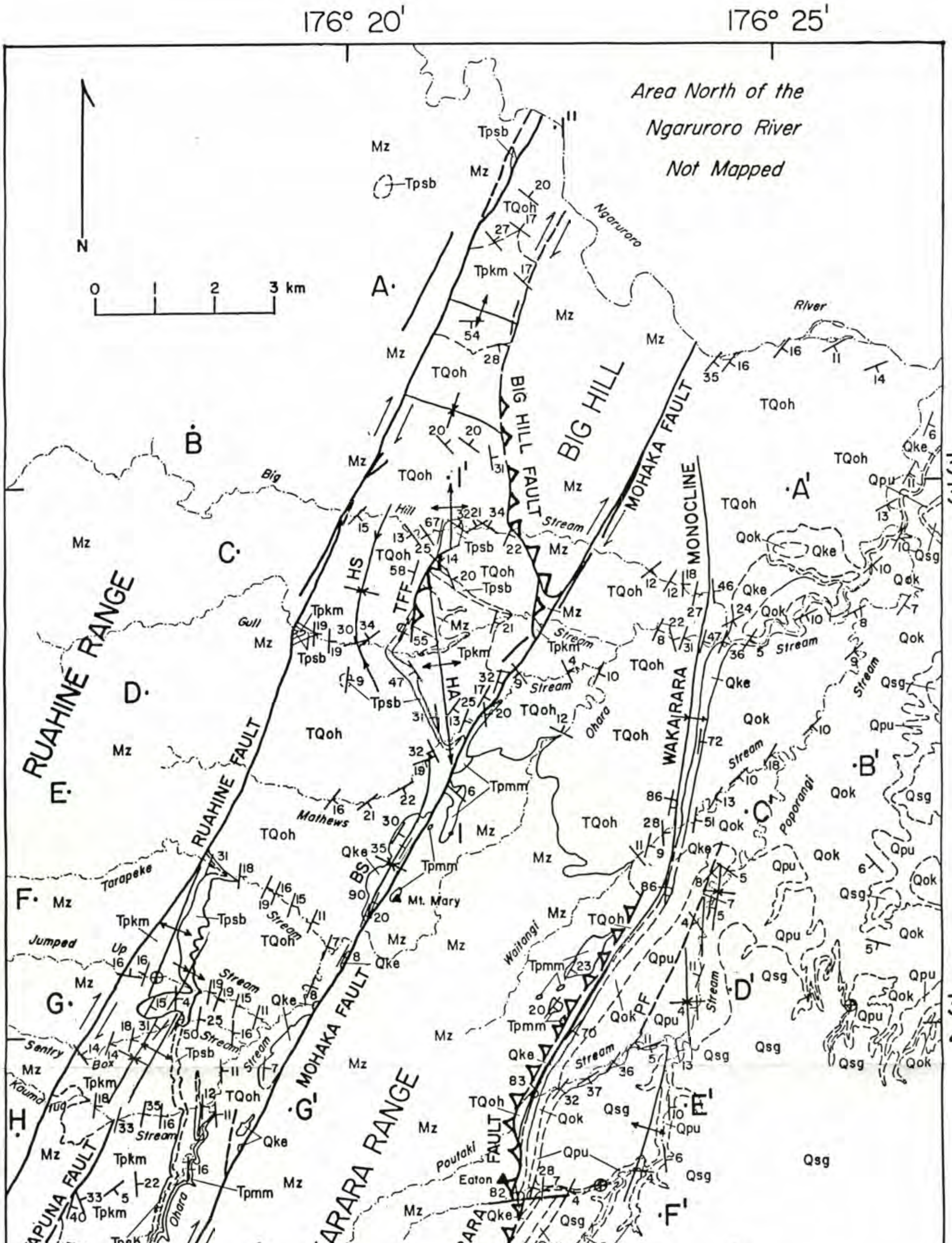

176° 20'
176° 25'
39° 35'
39° 40'
Area North of the Ngaruroro River Not Mapped
N
0 1 2 3 km
Ngaruroro River
Big Hill Stream
Gull Stream
Ohara Stream
Mathews Stream
Tarapeke Stream
Jumped Up Stream
Sentry Box Stream
Kauma Tua Stream
Waitangi Stream
Poutaki Stream
Poporangi Stream
Ohara
Poporangi
RUAHINE RANGE
RUAHINE FAULT
MATAPUNA FAULT
MOHAKA FAULT
BIG HILL
BIG HILL FAULT
WAKARARA MONOCLINE
WAKARARA FAULT
WAKARARA RANGE
Mt. Mary
Eaton
HS
TFF
HA
BS
PF
Not Mapped
A· A'
B B'
C· C'
D· D'
E· E'
F· F'
G· G'
H H'
I I'
Mz
Tpsb
Tpkm
TQoh
Tpmm
Qke
Qok
Qpu
Qsg

A sequence of early to middle Nukumaruan marine sediments crops out east of the Mohaka fault. The marine sediments are overlain by a middle Nukumaruan (early Pleistocene) to middle Castlecliffian(?) (middle Pleistocene) shallowing-upward sequence of marine to terrigenous deposits east of the Wakarara Range (Figures 2 and 3).

The purpose of this study is to investigate the deformational styles and tectonic history of the inboard strike-slip belt adjacent to the Ruahine Ranges of North Island, New Zealand. Studies in the southern Ohara Depression-Wakarara Range region by Raub (1985) prompted studies in the northern Ohara Depression, where the Plio-Pleistocene stratigraphy is well-exposed in stream canyons from the Mohaka fault to the Ruahine fault. Other geologic studies were reconnaissance only (e.g. McKay, 1877; Kingma, 1958; Stoneley et al., 1958; Grant-Taylor, 1978) or the studies were limited in their focus (e.g. Beu et al., 1977; Beu et al., 1980; Beu et al., 1981), therefore I defined and mapped the Plio-Pleistocene stratigraphy of the northern Ohara Depression-Wakarara Range region as a precursor to the investigation of deformational style and tectonic history. The stratigraphy is essential for understanding the structure, and changes in lithologies record the tectonic evolution of the Ohara Depression and the Wakarara Range region. The study focuses on the development of the Ohara Depression, the uplift of the Wakarara Range and the difference in

Figure 3) Generalized stratigraphic columns showing geology east and west of the Mohaka Fault. Mz, Torlesse Supergroup; Tpkm, Kaumatua Formation; Tpsb, Sentry Box Limestone; Tpmm, Mount Mary Limestone; TQoh, Ohara Mudstone, Waitangi Member east of the Mohaka Fault, Mangleton Member within the Ohara Depression; Qke, Kereru Limestone; Qok, Okauawa Formation; Qpu, Poutaki Pumiceous Formation; Qsg, Salisbury gravel lithofacies. Triangles indicate position of tephra layer or ignimbrite. Solid lines between contacts indicate certain correlation; dashed lines indicate probable correlation; dashed and queried lines indicate uncertain correlation.

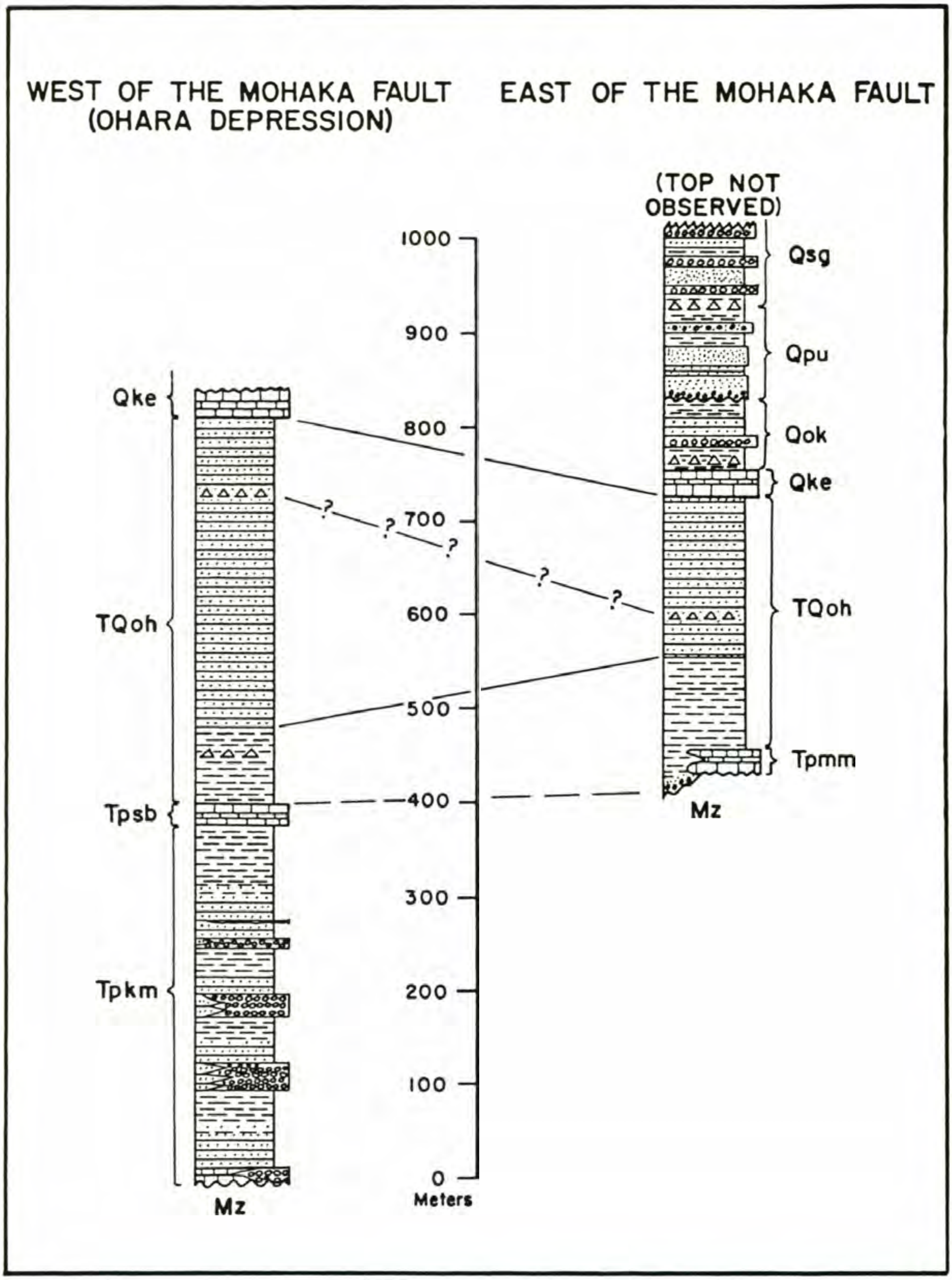

WEST OF THE MOHAKA FAULT
(OHARA DEPRESSION)
EAST OF THE MOHAKA FAULT
(TOP NOT OBSERVED)
Qsg
Qpu
Qok
Qke
TQoh
Tpmm
Mz
Qke
TQoh
Tpsb
Tpkm
Mz
1000
900
800
700
600
500
400
300
200
100
0
Meters

structural styles east and west of the Mohaka fault.

LITHOLOGIC UNITS

The Wakarara Range region was first visited by McKay (1877) who was primarily interested in the limestone beds and the relationship to Pliocene limestones to the east. Additional reconnaissance studies were done by Kingma (1958) and Stoneley et al. (1958). The southern Ohara Depression and southern Wakarara Range region were studied in more detail by Grant-Taylor (1978) and Raub (1985). My studies respond to many stratigraphic questions and problems in the northern Ohara Depression that have not been thoroughly addressed in previous studies.

The late Neogene units within and to the east of the Ohara Depression are typified by rapid lateral variations and, in some cases, complex interfingering of facies. Beds of conglomerate and limestone separate intervals of fine-grained clastics and can be good marker horizons. I recognize at least two different limestone sheets that are distinctive in lithology and time of formation (Figure 3). In addition, two isolated outcrops of limestone rest on Torlesse Supergroup rocks of the Ruahine Range. These limestone outcrops have an unclear relationship to the limestones within and to the east of the Ohara Depression.
The fine-grained sediments are differentiated by stratigraphic position relative to the most extensive limestones, by age, by association with conglomerates and, in some cases, by distinctive lithology. The ranges of age-diagnos-

Figure 4) The range of age-diagnostic micro- and macrofauna within the context of the New Zealand geologic time divisions and the European time divisions. New Zealand time divisions after Beu et al., (1986) and Edwards (1985, 1987). Faunal ranges after Beu at al., (1977), Beu et al., (1980), and A. Beu (personal communication, 1988, 1989). New Zealand stages: Wo, Opoitian; Wp, Waipipian; Wm, Mangapanian; Wn, Nukumaruan; Wc, Castlecliffian.

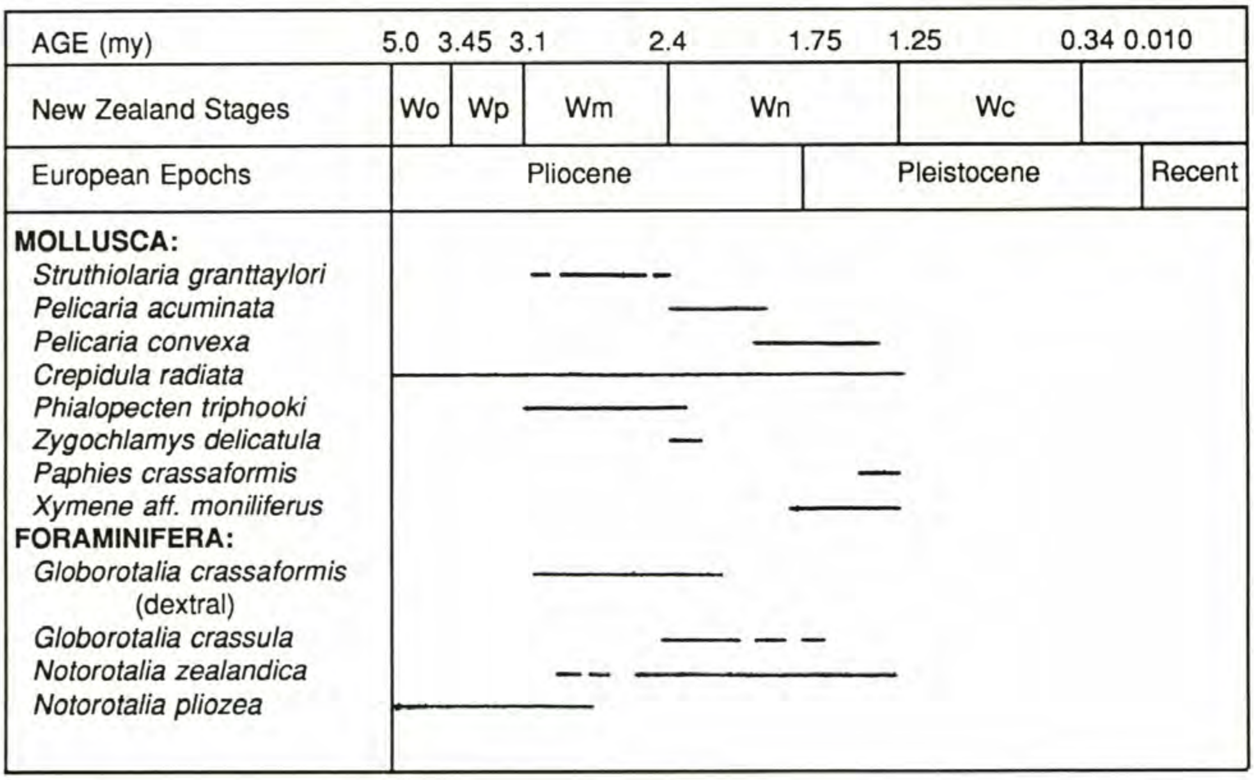
AGE (my)
5.0 3.45 3.1 2.4 1.75 1.25 0.34 0.010
New Zealand Stages
Wo
Wp
Wm
Wn
Wc
European Epochs
Pliocene
Pleistocene
Recent
MOLLUSCA:
Struthiolaria granttaylori
Pelicaria acuminata
Pelicaria convexa
Crepidula radiata
Phialopecten triphooki
Zygochlamys delicatula
Paphies crassaformis
Xymene aff. moniliferus
FORAMINIFERA:
Globorotalia crassaformis
(dextral)
Globorotalia crassula
Notorotalia zealandica
Notorotalia pliozea

tic fossils used in this study are shown in Figure 4.

Torlesse Supergroup

The basement in this region consists of the slightly metamorphosed, brittle and moderately to highly deformed rocks of the Torlesse Supergroup (Kingma, 1962). The Torlesse Supergroup consists of thick massive beds of fine to medium sandstone, alternating sandstone and argillite with local occurrences of red chert, and a melange of metavolcanics (Sporli and Bell, 1976; Raub, 1985). Torlesse Supergroup rocks in this area are Mid- to Upper Jurassic in age (Kingma, 1962; Speden, 1976; Te Punga, 1978).

Kaumatua Formation (New)

The Kaumatua Formation is a heterogeneous formation consisting of massive sandy mudstones, alternating interbeds of sandstone and mudstone, pebbly grainstones and conglomerate beds. The proposed type section of the Kaumatua Formation is in Kaumatua Stream, from the unconformable contact with the Torlesse Supergroup 50 m west of Mangleton Road, east to the base of the tan fine sandstone bed containing *Zygochlamys delicatula*. The Kaumatua Formation lies unconformably on the Torlesse Supergroup basement in all cases where I observed the lower contact. The Kaumatua Formation is a minimum of 100 m thick within the Ohara Depression. I have not observed it to the east of the Mohaka fault (Figure

2). In and south of Tarapeke Stream, the upper contact is gradational into the Sentry Box Limestone, farther north the contact is sharp and unconformable.

The sandstones are locally calcareous, fine-grained, micaceous, and slightly muddy, ranging from blue-grey to olive green where fresh, but weathering to tan. Following the system of Folk et al. (1970), these are litharenites. The mudstones are blue-grey and sandy, except where they crop out as 3-20 mm-thick, thinly laminated beds alternating with 30-100 mm sandstone beds. Limestones crop out as occasional 0.3 to 1 m-thick Ostrea beds and as 10-20 m-thick pebbly grainstones. Conglomeratic beds vary from 0.5-20 m thick, composed of matrix-supported to clast-supported granule- to cobble-size clasts. The clasts in the conglomerate beds are fine- to medium-grained sandstones, argillites, black chert and locally abundant red chert and metavolcanic fragments. Also present are layers of intraformational conglomerates. Fossils, either whole or as fragments, are also common in the conglomerate beds.

The age of the Kaumatua Formation is Mangapanian (late Pliocene) based on macro- and micro-fauna (Figure 5) (Beu et al., 1977; Alan Beu, personal communication, 1988). Some outcrops adjacent to the Ruahine Ranges may be Opoitian (Figures 4 and 5) (George Scott, personal communication, 1988).

Figure 5) Age ranges of the lithologic units of the Ohara Depression-Wakarara Range region based on the presence of age-diagnostic micro- and macro-fossil samples. New Zealand time divisions after Beu at al., (1986) and Edwards (1985, 1987). New Zealand stages: Wo, Opoitian; Wp, Waipipian; Wm, Mangapanian; Wn, Nukumaruan; Wc, Castlecliffian. Age assignments for macrofauna by A. Beu (personal communication, 1988, 1989), Beu et al., (1977), Beu et al., (1980), and Beu et al., (1981). Age assignments for microfauna from G. Scott (personal communication, 1988) and from Beu et al., (1977).

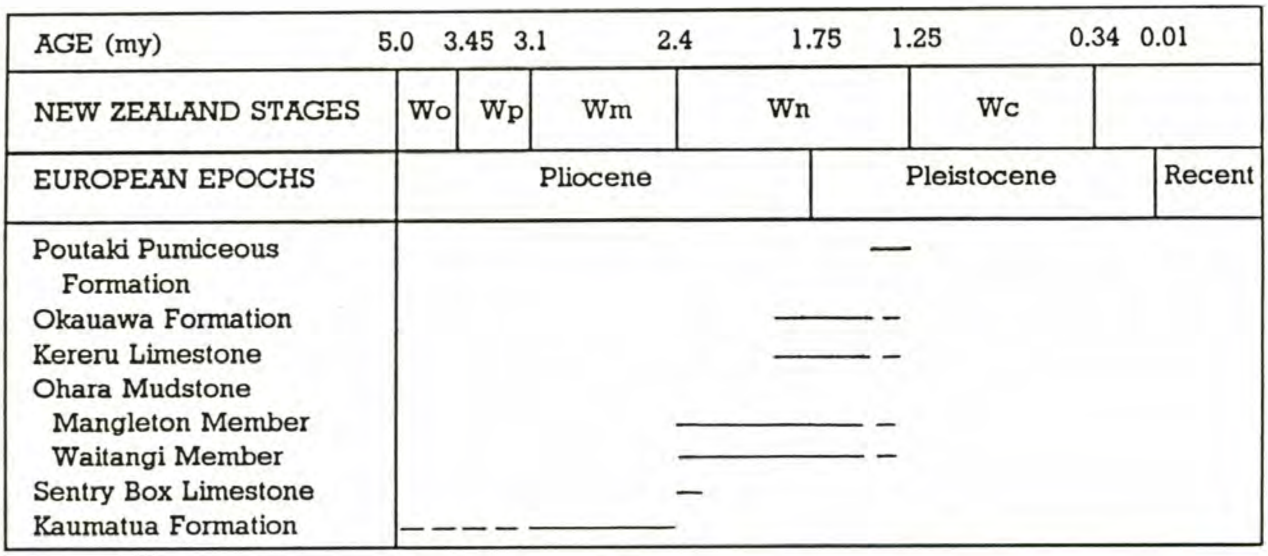
AGE (my)
5.0 3.45 3.1 2.4 1.75 1.25 0.34 0.01
NEW ZEALAND STAGES
Wo
Wp
Wm
Wn
Wc
EUROPEAN EPOCHS
Pliocene
Pleistocene
Recent
Poutaki Pumiceous Formation
Okauawa Formation
Kereru Limestone
Ohara Mudstone
Mangleton Member
Waitangi Member
Sentry Box Limestone
Kaumatua Formation

Sentry Box Limestone (New)

The Sentry Box Limestone varies from a pebbly, barnacle grainstone (classification of Dunham, 1962) to a fossiliferous mudstone-clast rudite (classification after Folk et al., 1970) with interbeds of massive mudstone and locally dominant granule to pebble conglomerates. Laterally the limestone grades into a tan to olive green fine sandstone containing *Z. delicatula*. The Sentry Box Limestone crops out most prominently between Sentry Box and Jumped Up Streams (Figure 2). The proposed type section is in Jumped Up Stream (New Zealand Map Grid (NZMG) U21/934666) (Figure 2), where the Sentry Box Limestone conformably overlies the Kaumatua Formation and grades upward into the Ohara Mudstone (Figure 3).

In the central to northern part of the study area, the pebbly barnacle grainstone (classification of Dunham, 1962) at Rocky Outcrop is correlative with the Sentry Box Limestone. Other lower Nukumaruan (upper Pliocene) barnacle grainstones and fossiliferous conglomerates within the Ohara Depression and adjacent to the Ruahine Range (Figure 2) are also included with the Sentry Box Limestone.

The typical thickness of the Sentry Box Limestone in these exposures is 20 to 25 m. The age of the Sentry Box Limestone is early Nukumaruan age (Beu et al., 1977; Beu et al., 1980) (Figure 5).

The barnacle grainstone preserved on the crest of the

Ruahine Range (Figure 2) (Kingma, 1962; Smale et al., 1978; Beu et al., 1981) is here correlated with the Sentry Box Limestone based on the similarity in lithology and the presence of *Z. delicatula.* Of less clear affinity is the recrystallized limestone resting unconformably on Torlesse Supergroup just south of the Ngaruroro River next to the active trace of the Ruahine fault (Figure 2). The original texture of the recrystallized limestone has been obscured because of proximity to the fault, but the limestone may be correlative in age with the Sentry Box Limestone to the south.

Mount Mary Limestone (New)

The Mount Mary Limestone is dominantly a pebbly, well-cemented grainstone based on the classification of Dunham (1962) and is composed of fragmental shells, bryozoa and other calcareous or aragonitic hard parts. Pebbles typically comprise 20-25% of the rock and are well-rounded and dominantly 3-15 mm in diameter. Most pebbles are light tan to dark brown, fine- to medium-grained sandstones and black argillite. Complete macrofossils are rare, with most bioclasts ranging from 2-10 mm.

In Mathews Stream at the crossing of the Mohaka fault (NZMG U21/984709) (Figure 2), the Mount Mary Limestone crops out as an impressive exposure of at least three sets of interbedded conglomerate and grainstone beds. The three 1 to 2 m-thick conglomerate beds contain rip-up clasts of poorly-indurated, laminated, muddy, very fine-grained sandstones and clasts of well-indurated fine sandstone cobbles and boulders to 0.30 m. Each conglomerate bed is overlain by well-cemented, fossiliferous, pebble conglomerates or pebbly grainstone beds. The conglomerate and grainstone beds grade upwards over a short stratigraphic interval (0.5-1 m) into a 5-10 m-thick massive mudstone with occasional granule to pebble layers and lenses as the Mount Mary Limestone interfingers with and grades into the overlying Ohara Mudstone.

Limestone beds deposited on the planated Torlesse Supergroup surface on the east and west flanks of the Wakarara Range (Figure 2) are correlative with the Mount Mary Limestone. The Mount Mary Limestone is absent where the Ohara Mudstone sits directly on Torlesse Supergroup basement. Maximum thickness of the Mount Mary Limestone is approximately 30 m. Though the section is not complete, the proposed type locality is at Mount Mary (NZMG U21/969681) where the greatest exposure of the limestone crops out. Because the limestone lies at or close to the base of the Ohara Mudstone, the Mount Mary Limestone is inferred to be early Nukumaruan (late Pliocene).

Ohara Mudstone (New)

The Ohara Mudstone consists of two members similar in thickness, lithology and age (Figures 5 and 6). The Waitangi Member crops out to the east of the Ohara Depression and the Mohaka fault and is a sequence of lower to middle Nukumaruan (upper Pliocene to lower Pleistocene) mudstone and fine sandstone. The Mangleton Member, of the same age (Figure 5), is a mudstone and sandstone that crops out in the Ohara Depression.

The Waitangi Member sits on the basement on the northern flanks of the Wakarara Range and both interfingers with and overlies the Mount Mary Limestone to the west in the area near Mathews Stream (NZMG U21/981704). The Waitangi Member is dominantly a blue-grey, micaceous, calcareous, very fine sandy mudstone approximately 318 m thick. Where it lies close to basement, the Waitangi Member contains 15-20% medium to coarse-grained particles of Torlesse Supergroup rocks, which rapidly decrease in size and abundance up-section. An interval of parallel-bedded muddy sandstone occurs near the base of the sequence (Figure 6), but overall, the mudstone is bioturbated and massive, with bedding commonly visible only as an alternating light and dark banding in weathered exposures. Up-section, the mudstone again becomes slightly sandier and bedding is more pronounced.

The Mangleton Member is approximately 412 m thick where it is exposed in Jumped Up Stream, above the 0.1-0.2 m thick gradational contact with the Sentry Box Limestone. The base

Figure 6) Stratigraphic sections of the lower massive mudstone of the Ohara Mudstone (dashed pattern) overlain by a well-bedded fine sandstone of the Ohara Mudstone (lined and stippled pattern). The sections indicate correlations and lateral variability of the coarse-grained and limestone facies and correlations of some of the tephras in the study area. Detailed measured sections from Jumped Up Stream and Waitangi Stream show the similarity in lithology of the lower Nukumaruan Ohara Mudstone east and west of the Mohaka Fault. Thicknesses of sections from other localities were determined from maps, cross sections and some field measurements. Note the similarity in thicknesses of the measured sequences from Jumped Up Stream and Waitangi Stream and the presence of a massive mudstone lithology in the lower portion. Solid lines indicate certain correlation of tephras (triangular pattern in sections) using tephra glass-chemistries determined by micro-probe analysis (Table 1); dashed lines indicate probable correlation based on stratigraphic position; dashed and queried lines indicate uncertain correlation. N.T.O., no tephra observed. Thick line indicates fault in section. Symbols of lithologic units as for Figures 2 and 3. Numbers at the base of each section indicate the accuracy of the stratigraphic thickness shown: 1, best: detailed measured section using tape and brunton or measuring staff; 2, intermediate: thickness determined by pace and brunton or other rough estimates in the field, stratigraphic thickness from cross section or map with good structural control; 3, lowest quality: uncertainties due to lack of structural control.

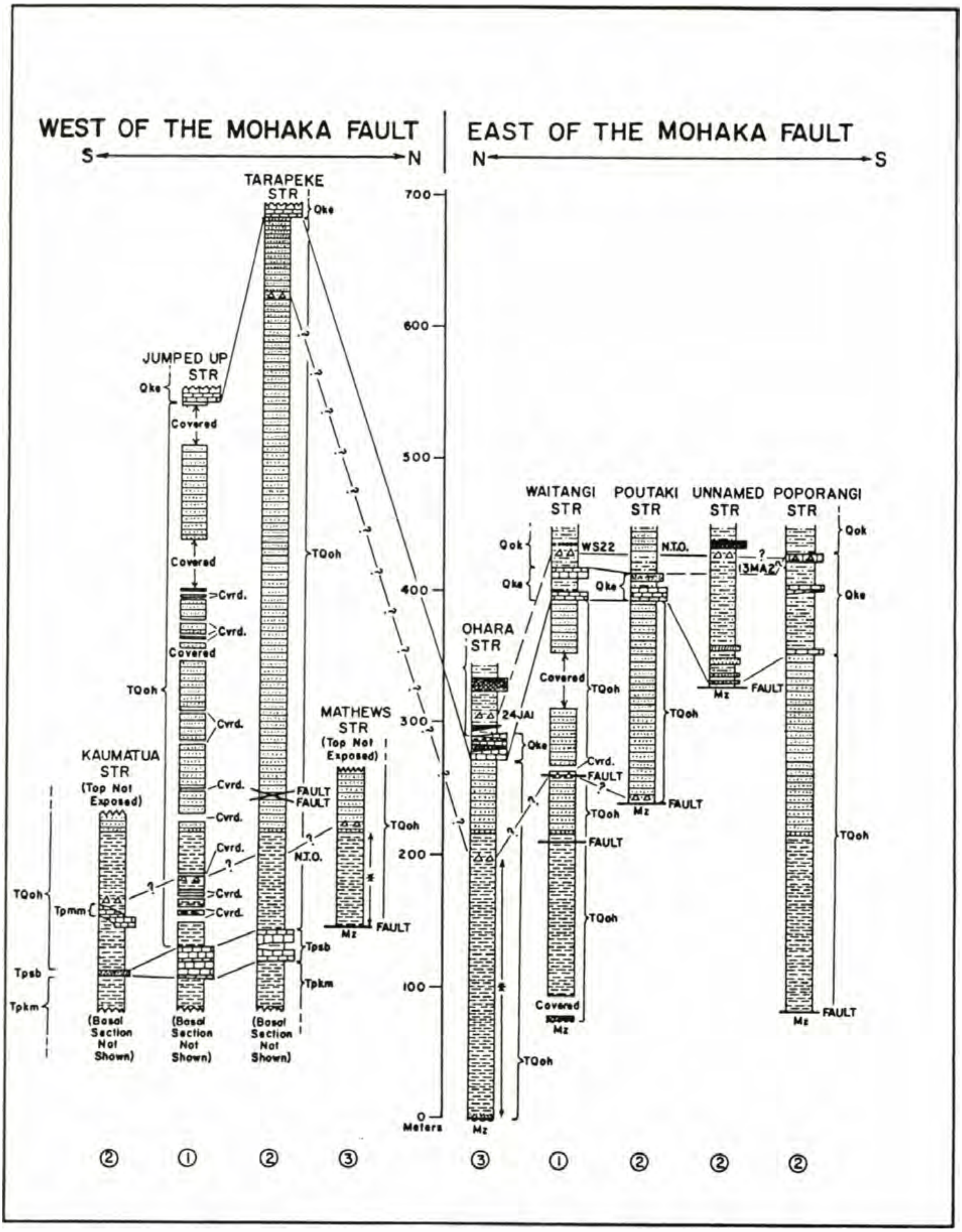

WEST OF THE MOHAKA FAULT
S
N
EAST OF THE MOHAKA FAULT
N
S
TARAPEKE STR
JUMPED UP STR
KAUMATUA STR
(Top Not Exposed)
MATHEWS STR
(Top Not Exposed)
OHARA STR
WAITANGI STR
POUTAKI STR
UNNAMED STR
POPORANGI STR
Qke
Qok
TQoh
Tpmm
Tpsb
Tpkm
Covered
Cvrd.
FAULT
N.T.O.
WS22
13MA2
24JA1
Mz
(Basal Section Not Shown)
Meters
0
100
200
300
400
500
600
700
②
①
②
③
③
①
②
②
②

of the Mangleton Member is a massive mudstone 80 m thick (Figure 6), which grades into interbedded sandstone and mudstone over 2-3 m. The sandstone beds are 20-300 mm thick and alternate with finely laminated mudstone and claystone layers 5-30 mm thick. The sandstones are a blue-grey, locally fossiliferous and bioturbated, micaceous, weakly to moderately calcareous litharenite using the classification of Folk et al. (1970). The mudstone and claystone layers are distinctively more calcareous and are locally disrupted by burrows.

At least two tephras are present in the Mangleton Member of the Ohara Mudstone (Figures 3 and 6). Only tephras along the east front of the Wakarara Range have been correlated by micro-probe analysis of glass chemistry (Brad Pillans, personal communication, 1989) (Table 1 and Figure 6). One tephra, approximately 80 m below the Ostrea-rich limestone beds on the western flank of the Wakarara Range (Figures 3 and 6) is tentatively correlated based on stratigraphic position with a tephra in the Waitangi Member approximately 130 m below the Kereru Limestone (Figure 6). The absence of a tephra layer near the base of the Waitangi Member, which would correspond to the other tephra in the Mangleton Member 50 m above the Nukumaruan Sentry Box Limestone (Figure 6), suggests that the base of Waitangi Member is slightly younger.

For the type section for the Ohara Mudstone, I propose

TABLE 1. Correlated tephras and their glass chemistries (weight % oxides).

Sample[1]	SiO_2	Al_2O_3	FeO	MgO	CaO	Na_2O	K_2O
WS22	76.32	13.03	1.13	0.11	1.07	3.79	4.21
13MA2	76.91	12.77	1.07	0.14	1.00	3.62	4.24
24JA1	77.45	12.42	1.12	0.11	1.05	3.59	3.93

[1] Locations of samples on Figure 6.

the exposure of the Mangleton Member that extends along approximately 1 km of the channel of Jumped Up Stream and also extends up the cliff face at the confluence of Jumped Up Stream with Ohara Stream. The section is continuous to the base of the overlying Kereru Limestone.

Kereru Limestone (Emended From McKay, 1877)

The Kereru Limestone was first investigated by McKay (1877) who noted the prominent ridge of limestone to the west of Kereru Station. McKay (1877) also referred to the limestones sitting on the northern flanks of the Wakarara Range and the Sentry Box Limestone as Kereru Limestone, but based on paleontology, lithology and my detailed mapping, the Mount Mary Limestone and the Sentry Box Limestone are older (Figures 3 and 5) and were deposited in environmental settings different from that of the Kereru Limestone. The Kereru Limestone consists of distinctive muddy to densely packed beds of Ostrea and, locally, other shells, as well as calcarenites and hard calcareous-cemented, fine to medium-grained litharenites (classification of Folk et al., 1970). Up to 25% of the bioclastic beds consist of pebbles derived from the basement rocks. Where large clastic particles do occur, they are well-rounded pebbles usually 3-20 mm, with some clasts up to 150 mm.

The beds of limestone interfinger with blue-grey massive sandy mudstones, fine, parallel-bedded tan sands, and to the north interfinger with weakly calcareous conglomerates (Figure 6). The Kereru Limestone laterally grades northward into a fine, massive to laminated, muddy sandstone in the lower reaches of Ohara Stream and Poporangi Stream (Figure 2).

Okauawa Formation (New)

The Okauawa Formation is exposed to the east of the Mohaka fault above the last grainstone bed of the Kereru Limestone. It consists of blue-grey to green, 20-200 mm-thick interbeds of fine sandstone and mudstone, massive mudstones, shell conglomerates, and granule to pebble conglomerates. Mudstone:sandstone:conglomerate ratios range from 2:1:0 to 1:1:1 in the lower 50-75 m and range from 1:1:0 to 2:1:0 higher up. Mudstone and claystone beds of this unit tend to be calcareous, but less so than the Ohara Mudstone.

The conglomerates, where present, crop out only near the base of the Okauawa Formation in the vicinity of the contact with the Kereru Limestone (Figure 6). Clasts are rounded to well-rounded, and are composed mostly of tan to black fine sandstones, argillites and chert. Fossil fragments are common in the conglomerate beds. Conglomerates are absent in Poutaki Stream (Figure 2). Thick conglomerate beds of nearly 15 m crop out in the lower reaches of Ohara Stream (McKay, 1877; Kingma, 1958), where they interfinger with and overlie the Kereru Limestone.

The Okauawa Formation has a minimum thickness of 100 m along the east front of the Wakarara Range, but may thicken to the east outside of the study area. Within the study area, it is unconformably overlain by the Poutaki Pumiceous Formation. The age of the Okauawa Formation is middle to late Nukumaruan (early Pleistocene) (Figure 5). The proposed type locality for the Okauawa Formation is along Okauawa Stream to the east of the study area, where part of the formation was measured and studied by Clark (1976). The best exposure of the lower coarse-grained facies is in Waitangi Stream, stratigraphically above the last grainstone bed of the Kereru Limestone to a point about 100 m downstream.

Poutaki Pumiceous Formation (New)

The base of the Poutaki Pumiceous Formation is a 1-1.5 m thick pumiceous sandstone bed (pumice litharenite of Folk et al. (1970)) containing rip-up clasts of mudstone and sandstone lying unconformably on the Okauawa Formation. Also present at or within 0.3 m of the basal unconformity at some localities is a 0.3-1.0 m thick bed of grainstone (classification of Dunham, 1962).

Above the basal pumiceous sandstone, the Poutaki Pumiceous Formation consists of coarse pumiceous sandstone beds, pumiceous granule to cobble conglomerates, dark green medium-grained sandstone beds, alternating 10-50 mm thick beds of fine sandstone and mudstone, and massive mudstone. Also present are lignite bands, tree trunks and other carbonaceous matter. Individual beds may be non-pumiceous, but even the mudstone layers often contain pumiceous clasts to 30 mm. This unit is distinctly non-calcareous, except in some massive mudstone and claystone beds.

The only fossils recovered from this unit were found several kilometers to the east, which indicate a late Nukumaruan age for this unit (Figure 5) (Alan Beu, personal communication, 1989). The Poutaki Pumiceous Formation coarsens upward into the Salisbury gravel lithofacies.

The proposed type section is in Poutaki Stream, at NZMG U21/007653, where the lower unconformity is exposed. Near the top of the cliff at this locality, the Poutaki Pumiceous formation is overlain by a 6 m thick ignimbrite which is defined as the beginning of the Salisbury gravel lithofacies. The Poutaki Pumiceous Formation is a minimum of 60 m thick within the study area, and up to 100 m thick farther east.

Salisbury Gravel Lithofacies

The Salisbury gravel lithofacies is poorly exposed in the study area. The lower contact is mapped at the first distinct ignimbrite bed. Otherwise, the lower part of the unit is difficult to distinguish from the Poutaki Pumiceous Formation, because the Salisbury gravel lithofacies also contain massive mudstone beds interbedded with pumiceous sandstones and conglomerate beds. To the east of the field area, I observed that pebble to cobble conglomerates of the Salisbury gravel lithofacies become prevalent up-section, with interbeds of pumiceous sandstone and more ignimbrites. The Salisbury gravel lithofacies are nonfossiliferous, and I infer that their age range is late Nukumaruan(?) to early Castlecliffian (middle Pleistocene).

STRUCTURE

The structures in and around the Ohara Depression are dominated by basement uplifts. Because late Neogene sediments within the Ohara Depression are less than 1 km thick, the sediments are sensitive to movements in the basement blocks. Folding and faulting of the late Neogene units are commonly associated with faults within the basement. Folds are commonly abrupt, as reflected by abrupt changes from shallowly dipping strata to nearly vertical or overturned strata within a few hundred meters.

The four basement blocks in the study area are the Big Hill block, the Wakarara block, the Ruahine block and the Ohara block (Figure 7). Deformation of the basement blocks and the overlying deposits is shown in a structure contour map of the area (Figure 8). I constructed Figure 8 using the base of the early Nukumaruan Ohara Mudstone as the contoured surface both east and west of the Mohaka fault. In areas where the Ohara Mudstone is absent, the planated Torlesse Supergroup surface is contoured. With the exception of the Big Hill block, the planated Torlesse surface was exposed in the early Nukumaruan, though the surface may not have been cut at that time. The structural contour map therefore portrays vertical movement of the various blocks as well as folding of the Plio-Pleistocene rocks.

Structures along the east front of the Wakarara Range are clearly contractional and the structures within the

Figure 7) Tectonic sketch map of the study area and the Ruahine Range front showing megascale folds and faults. Stippled pattern, Mesozic Torlesse Supergroup; BHF, Big Hill fault; HS, Herricks syncline; HA, Herricks anticline; TFF, Thorn Flat fault; BS, Balcony syncline; WAM, Wakarara monocline; WAF, Wakarara fault; PF, Poporangi fault; YS, Yeoman's syncline; CF, Cullens fault; HF, Hylton fault; TT, Tukituki Thrust. After Grindley (1960), Kingma (1962), Grant-Taylor (1978), Raub (1985) and Browne (1986).

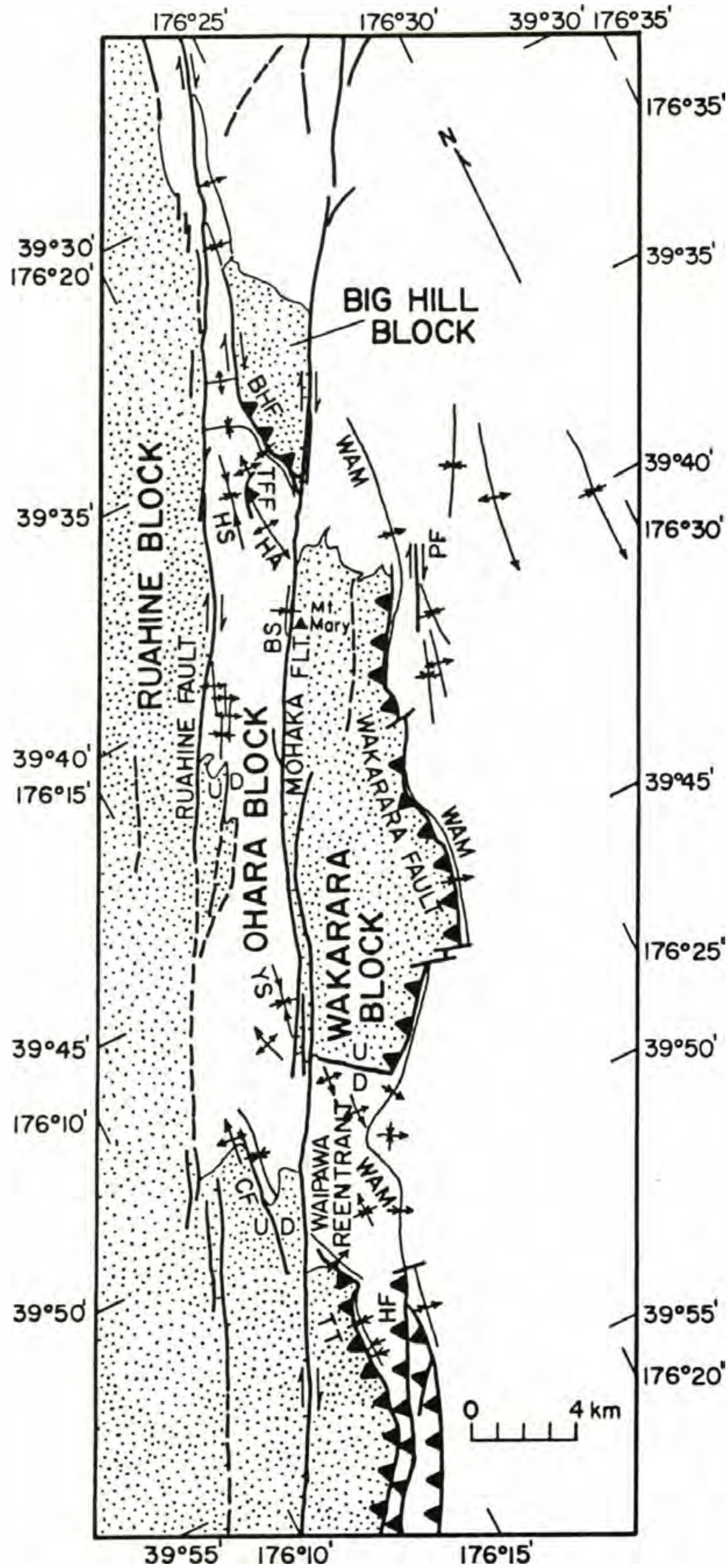

176°25'
176°30'
39°30' 176°35'
176°35'
N
39°30'
176°20'
39°35'
BIG HILL
BLOCK
BHF
TFF
SH
HA
WAM
PF
39°40'
39°35'
176°30'
RUAHINE BLOCK
RUAHINE FAULT
BS
Mt. Mary
MOHAKA FLT
WAKARARA FAULT
39°40'
176°15'
OHARA BLOCK
39°45'
WAM
176°25'
YS
WAKARARA BLOCK
39°45'
39°50'
U
D
176°10'
WAIPAWA REENTRANT
WAM
CF
U
D
39°50'
HF
39°55'
176°20'
0
4 km
39°55'
176°10'
176°15'

Figure 8) Structural contour map using the top of the Sentry Box Limestone and the equivalent stratigraphic horizon within the Ohara Depression as the contoured surface. East of the Mohaka Fault, the topographically-defined Torlesse Supergroup planation surface and the base of the Ohara Mudstone is the contoured surface. All of these surfaces are approximately early Nukumaruan (c.a. 2.0-2.4 my) in age. HA, Herricks anticline; HS, Herricks syncline; TFF, Thorn Flat fault; BS, Balcony syncline; WAM, Wakarara monocline; MPF, Matapuna fault; PF, Poporangi fault.

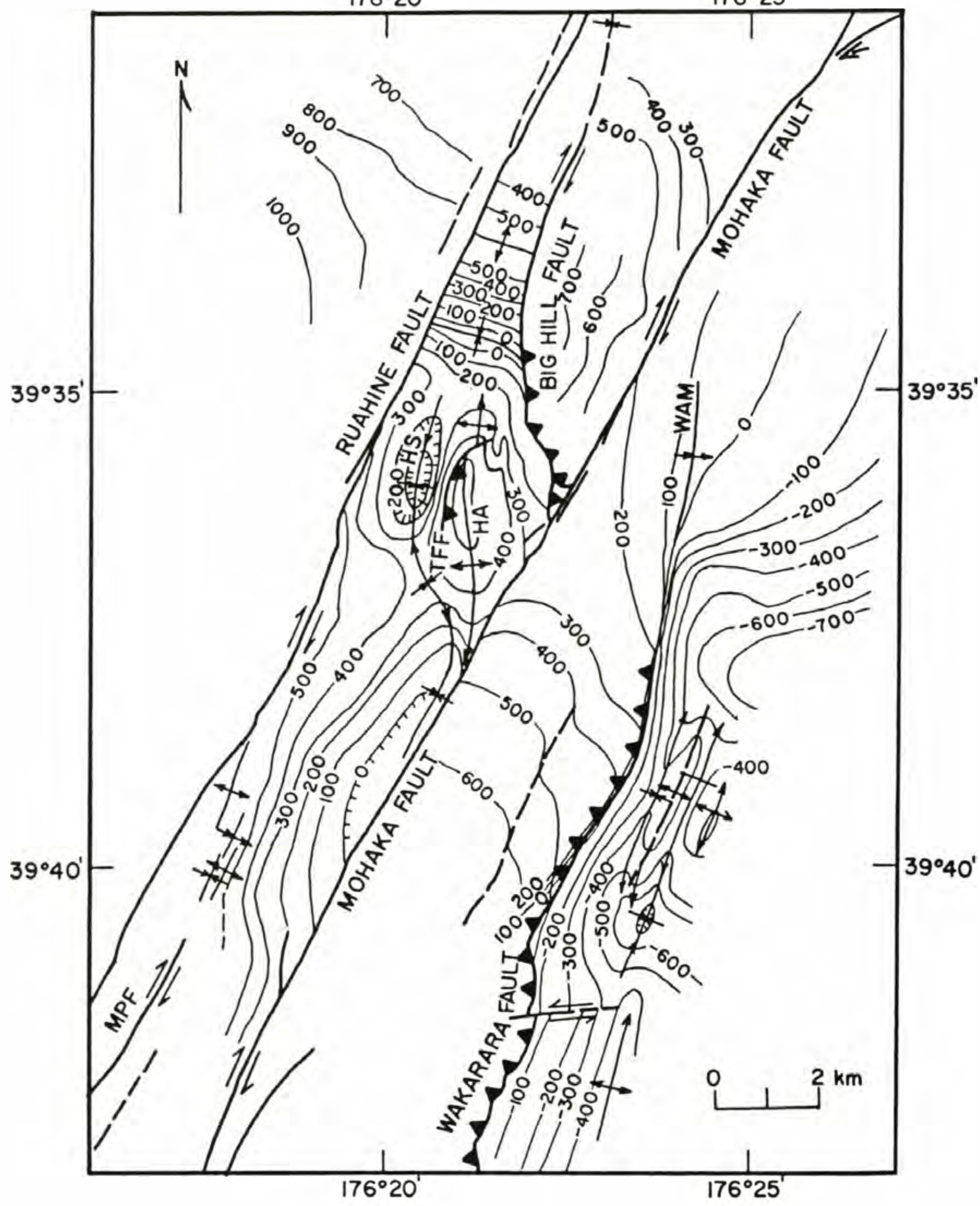
176°20'
176°25'
39°35'
39°40'
N
RUAHINE FAULT
BIG HILL FAULT
MOHAKA FAULT
WAKARARA FAULT
MPF
WAM
HS
HA
TFF
0 2 km

Ohara Depression are dominantly related to dextral strike-slip faulting on the Mohaka and Ruahine faults (Figures 7 and 8). Because of the differences in styles of folding and faulting, I have divided the area into two structural domains. The first domain, the Ohara Depression domain, is bounded on the northwest and southeast by the Ruahine and Mohaka faults, respectively. The second domain, the Wakarara domain, is the region east of and including the Wakarara fault and Wakarara monocline.

Division of the area into two structural domains is supported by the stress tensor analysis of striated faults. Using the method and program of Angelier (1984), I determined the orientation of the maximum, minimum and intermediate stress directions for the Ohara Depression domain and the Wakarara domain (Figure 9). Though the two domains have similar maximum compressive directions, they differ in the orientation of the intermediate and minimum stress directions (Figure 9).

Deformation Related to the Ohara Depression Domain

Within the Ohara Depression, several subdomains of folding and faulting are defined. In the southern part of the study area, the large-scale structure is a homocline, with strata dipping gradually to the east-southeast (Figures 2 and 8 and Figure 10, cross sections E through H). Contractional structures dominate to the north, adjacent to the

Figure 9) Tectonic map of Ohara Depression and Wakarara region showing measurement sites for megascale and mesoscale fault data. Fault data are separated into an Ohara Depression domain (stereonet A) and a Wakarara domain (stereonet B). For each stereonet: great circles, faults; open circles, striation lineations; crosses, the maximum, intermediate and minimum stress directions (σ_1, σ_2 and σ_3). Principal stresses calculated by the stress tensor analysis method of Angelier (1984).

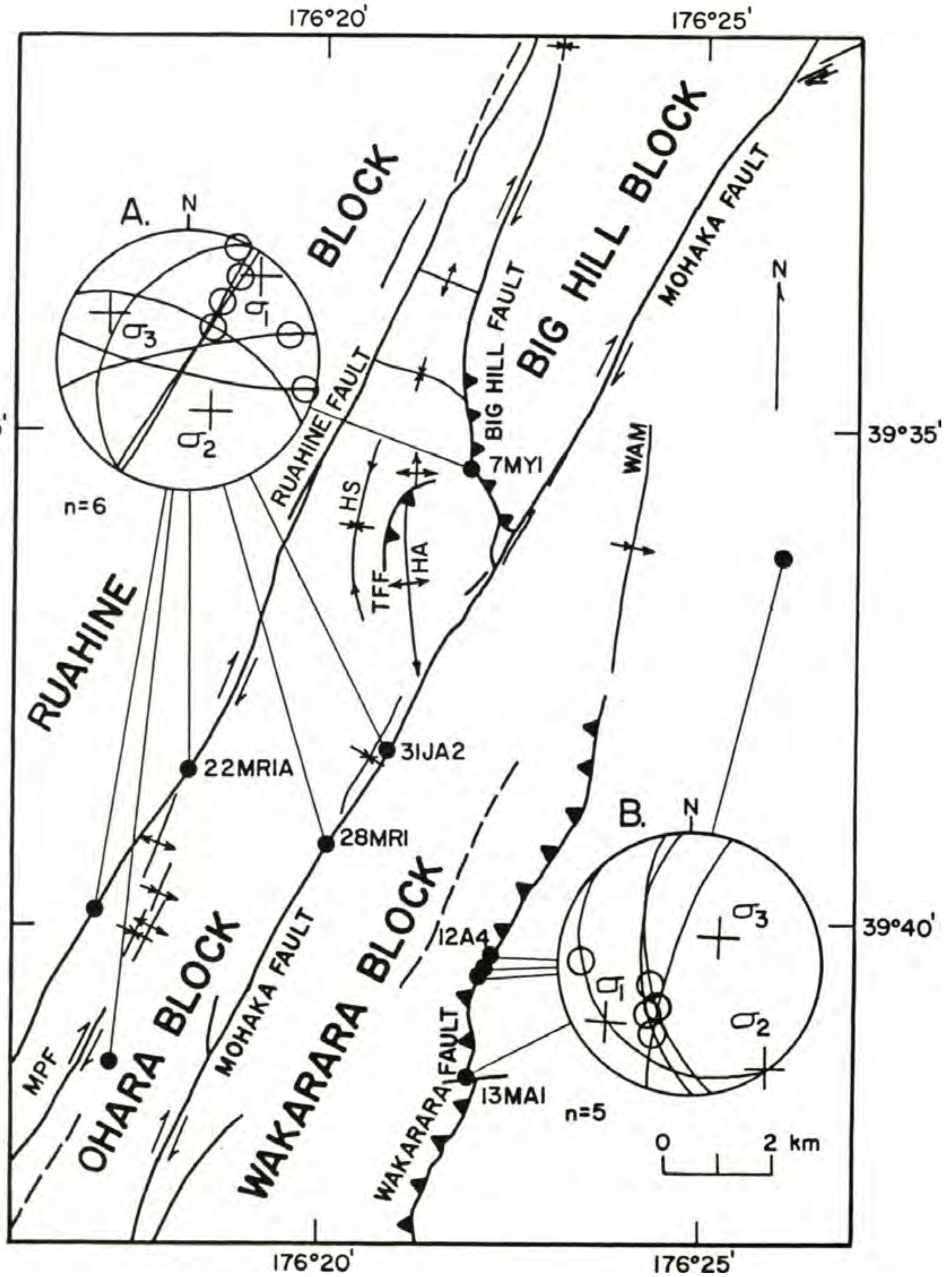
176°20'
176°25'
39°35'
39°40'
BLOCK
BIG HILL BLOCK
MOHAKA FAULT
BIG HILL FAULT
RUAHINE FAULT
A.
N
n=6
7MYI
HS
HA
TFF
WAM
RUAHINE
22MRIA
31JA2
28MRI
B.
n=5
12A4
13MAI
OHARA BLOCK
WAKARARA BLOCK
WAKARARA FAULT
MPF
0
2 km

Figure 10) Structural cross sections of the Ohara Depression and Wakarara Range front. Location of cross section lines shown on Figure 2. Mz, Torlesse Supergroup; Tpkm, Kaumatua Formation; Tpsb, Sentry Box Limestone; Tpmm, Mount Mary Limestone; TQoh, Ohara Mudstone; Qke, Kereru Limestone; Qok, Okauawa Formation; Qsg, Salisbury gravel lithofacies; RF, Ruahine fault; MF, Mohaka fault; MPF Matapuna fault; TFF, Thorn Flat fault; BHF, Big Hill fault; WAF, Wakarara fault.

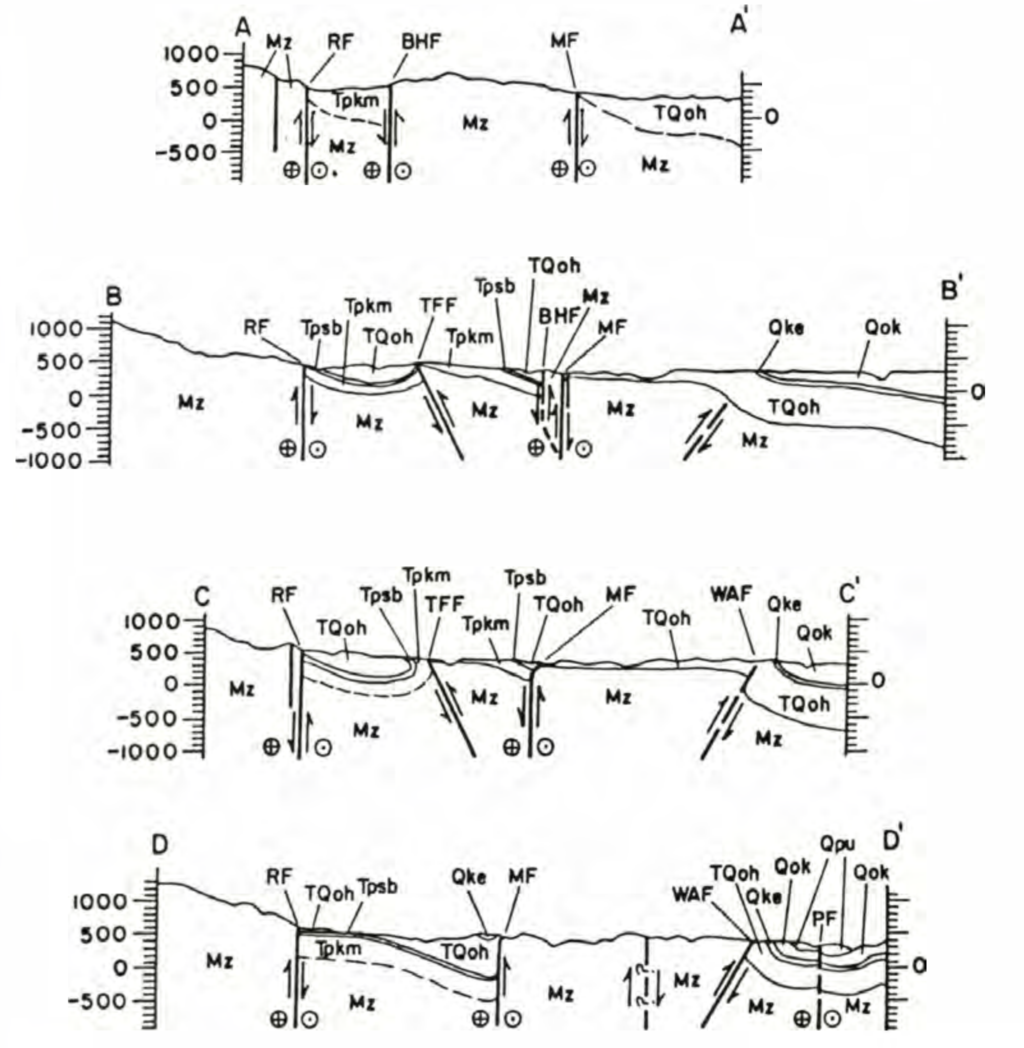
A
A'
Mz
RF
BHF
MF
Tpkm
TQoh
Mz
B
B'
TQoh
Tpsb
Tpkm
TFF
BHF
Qke
Qok
C
C'
WAF
Qke
Qok
D
D'
Qke
Qok
Qpu
PF
1000
500
0
-500
-1000

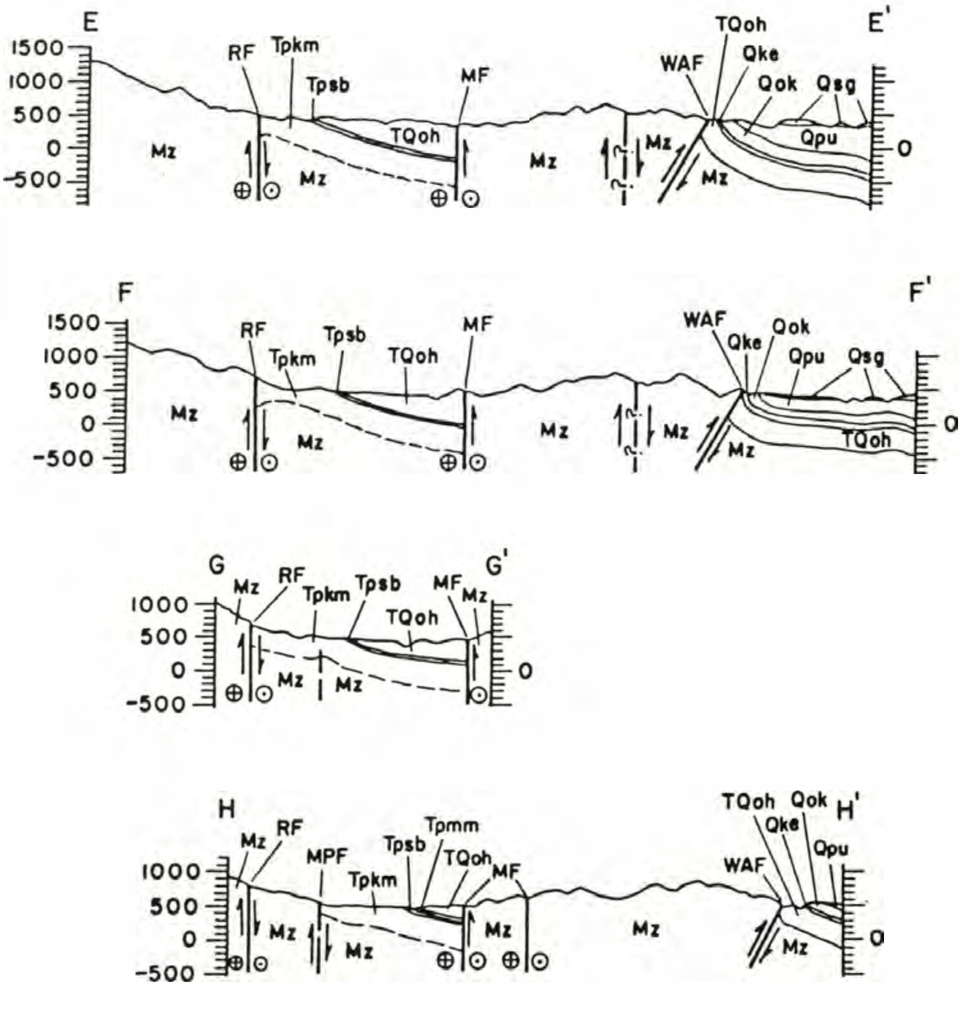
E
E'
1500
1000
500
0
-500
RF
Tpkm
Tpsb
MF
TQoh
Mz
WAF
Qke
Qok
Qsg
Qpu
F
F'
RF
Tpkm
Tpsb
TQoh
MF
WAF
Qke
Qok
Qpu
Qsg
G
G'
RF
MF
H
H'
MPF
Tpmm

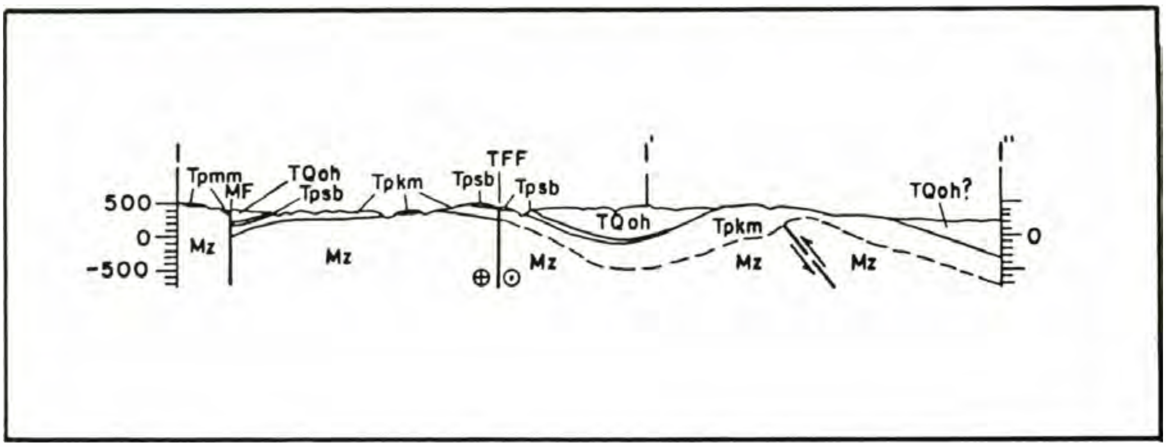

I
Tpmm
MF
TQoh
Tpsb
Tpkm
Tpsb
TFF
Tpsb
I'
TQoh
Tpkm
I''
TQoh?
500
0
-500
Mz
Mz
Mz
Mz
Mz
0

Big Hill fault (Figures 7 and 8). The structural differences between the northern and southern parts of the study area are also evident in the cumulative horizontal shortening measured along lines trending S60E (Figure 11, line C versus lines D and F).

The Ruahine fault is a dextral strike-slip fault that trends 020-030° through the study area. In the only good exposure of the fault, in Tarapeke Stream, the fault is vertical (Table 2) and elsewhere is inferred to be high-angle from the map pattern. The Ruahine fault can be divided into four segments (Table 3). The northern segment may be the Glenn Ross fault as mapped farther to the north by Browne (1986), bending into the Ruahine fault, or middle segment, approximately 1 km south of the Ngaruroro River (Figure 2). Net northwest-side-up vertical movement on the Ruahine fault since the early Nukumaruan increases to the south (Table 3 and Figure 10, cross sections A and F). The most recent movement, however, has been southeast-side up. Striations on the fault surface in Tarapeke Stream (Table 2) are consistent with the southeast side up and dextral strike-slip faulting.

There are no significant markers for determining the total strike-slip offset along the Ruahine fault. The predicted coast-parallel movement between the Pacific and Australian plates (along a trend of about 027°) since the beginning of the Nukumaruan (2.4 my BP) would be 62 km,

Figure 11) Cumulative shortening (km/km) across the Ohara Depression and Wakarara area along the eight cross section lines shown in Figure 2. All lines trend S60E. HA, Herricks anticline; HS, Herricks syncline; WFFB, Wakarara fold and fault belt.

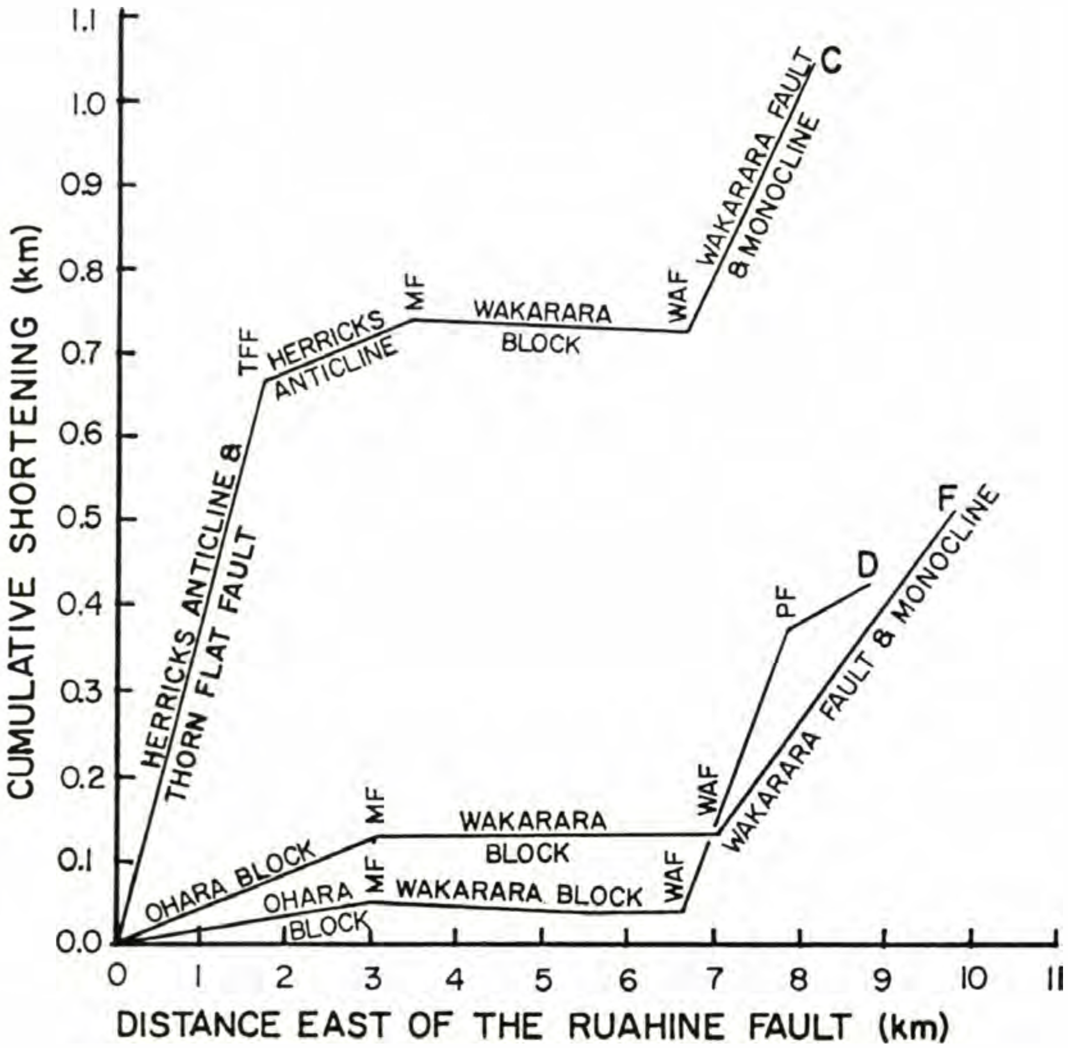
CUMULATIVE SHORTENING (km)
DISTANCE EAST OF THE RUAHINE FAULT (km)
HERRICKS ANTICLINE &
THORN FLAT FAULT
TFF
HERRICKS
ANTICLINE
MF
WAKARARA
BLOCK
WAF
WAKARARA FAULT
& MONOCLINE
C
OHARA BLOCK
MF
WAKARARA
BLOCK
WAF
PF
D
F
WAKARARA FAULT & MONOCLINE
OHARA
BLOCK
MF
WAKARARA BLOCK
WAF

Table 2. Orientation of major faults with slip indicators in the Ohara Depression-Wakarara Range region.

Fault	Site ID[1]	Fault orientation[2]		Lineation orientation[3]		Description of lineation
		S	D	T	P	
Ruahine (southern segment)	22MR1A	32	90	32	25	gouge w/striae
Big Hill	7MY1	120	63NE	37	60	gouge w/striae
Mohaka (mid-southern segment)	28MR1	29	89SE	30	47	gouge w/striae
Mohaka (mid-northern segment)	31JA2	120	40NW	24	6	offset ridges
Wakarara	12A4	18	79NW	211	58	gouge w/striae
Wakarara	12A4	177	59NW	205	39	gouge w/striae
Wakarara	12A4	177	59NW	242	56	gouge w/striae
Wakarara	13MA1	170	64NW	241	63	gouge w/striae

[1] See Figure 9 for site location.

[2] S, strike; D, dip.

[3] T, trend; P, plunge.

TABLE 3. Segments along the Ruahine fault.

Segment location	Segment length (km)	Diagnostic features	Holocene scarps	Observed striae[1]	Horiz:Vert offset
northern[2]	10+[3]	southeast up vertical fault(?)	yes	none	n/a
northern middle	3	northwest up	no	none	n/a
middle	7	northwest up a min. of 200 m, vertical fault(?), rectilinear map pattern	yes	none	n/a
southern[2]	16+[3]	vertical to northwest-dipping(?) fault, northwest up	yes/ obscure to south	yes	2.1:1

[1] See Table 2 for orientations of faults with slip indicators.

[2] Fault segment extends outside of study area.

[3] Minimum length of segment given, including portions outside of the study area.

using the present-day Antarctic-Pacific finite rotation pole of Gordon et al., (1988). This gives a maximum horizontal slip for the Ruahine fault or any combination of faults in the forearc region for the last 2.4 my. Beu (1977) suggests a correlation of rock units at Mangleton Road in the Ohara Depression with those at Mt. Miroroa; this correlation implies 20 km of horizontal dextral offset along the Ruahine fault since the early Nukumaruan. Assuming that the late Quaternary slip-rate estimates of Beanland and Berryman (1987) of 1.0-2.0 mm/yr are valid back to the early Nukumaruan, dextral strike-slip since the early Nukumaruan would be on the order of 2.4 to 4.8 km.

Adjacent to the Ruahine fault, beds dip moderately to the east in most cases. However, in Jumped Up Stream, the beds dip gently to the northwest forming a north-trending anticline (Figure 10, cross section F). In Tarapeke Stream, nearly vertical late Tertiary beds next to the main fault trace consist of a 5 m thick phacoid, having a fault-contact with other late Tertiary beds to the east.

The Mohaka fault trends approximately 030° through most of the study area. The fault is predominantly a vertical right-lateral strike-slip fault (Table 2 and Figure 10, cross sections A,B and E through H). The Mohaka fault can also be divided into several segments (Table 4). The most notable difference among the segments of the Mohaka fault is that the net vertical movement along the Mohaka fault in-

TABLE 4. Segments along the Mohaka fault.

Segment location	Segment length	Diagnostic features	Holocene scarps	Observed striae[1]	Horiz:Vert offset
northern[2]	11[3]	northwest up a min. of 200 m, vertical fault	yes	none	n/a
mid-northern	5	40-45° NW dip, minor vertical offset	yes	none	8:1
mid-southern[2]	17	vertical fault, southeast up approx. 1 km	yes/obscure	yes	≥1:1
southern[2]	13	vertical fault(?), southeast up approx. 1 km[4]	yes	none	n/a

[1] See Table 2 for fault orientations with slip indicators.

[2] Fault segment extends outside of study area.

[3] Minimum length of fault segment given, including portions outside of the study area.

[4] Vertical offset across both the mid-southern and southern segments.

creases from north to south and the vertical slip changes from northwest side up in the northern segment to the southeast side up in the southern two segments (Table 4). I interpret the mid-northern segment (Table 4) to be a transitional segment between the northern and mid-southern segments, accommodating both a slight right-step and reversal in the sense of vertical slip (Figure 2 and Figure 10, cross sections B through D).

The Mohaka fault is also similar to the Ruahine fault in that lack of appropriate markers precludes determination of the net horizontal displacement since the early Nukumaruan (2.4 my BP). If the late Quaternary slip rates determined by Hull (1983, 1985) of 3.0-4.0 mm/yr and Raub (1985) of 3.0 mm/yr are extrapolated back through the early Nukumaruan, the total horizontal slip on the Mohaka fault would be in the range of 7.2 to 9.6 km.

Along the west side of the mid-northern and mid-southern segments of the Mohaka fault, the Nukumaruan strata dip gently to the east or are openly folded near Mount Mary into the Balcony (informal local name) syncline (Figure 2 and Figure 10, cross section D). The bedding is vertical near the southern end of Mount Mary, but becomes gently east-dipping only 1 km to the south along the Mohaka fault (Figure 2).

Uplift of the Big Hill block along the northern segment of the Mohaka fault has resulted in minor deformation on the east side of the Mohaka fault. Beds dip at low to moderate angles to the east in the exposures at the Ngaruroro River and in Mathews Stream (Figure 2 and Figure 10, cross sections A and B). In Big Hill Stream, the only visible bedding is folded into a 1 m-long syncline next to the fault. In Gull Stream, the Ohara Mudstone dips steeply (42°) and homoclinally to the east between two splays of the Mohaka fault (Figure 2).

The Big Hill block has a poorly preserved planation surface on the east flank of Big Hill. On the north side of the Ngaruroro River, the planation surface is better preserved and forms the contact between the Mangapanian unit and the Torlesse Supergroup (Kingma, 1958; Beu et al., 1980). Though the planation surface is Mangapanian rather than early Nukumaruan, the surface does approximate the style of deformation of the Big Hill block (Figure 8). Movement along the Big Hill fault is largely responsible for the uplift of the Big Hill block and tilt to the northeast and southeast (Figure 8).

The Big Hill fault extends from the Mohaka fault in the vicinity of Gull Stream, along the west side of Big Hill and to the north side of the Ngaruroro River. The surface exposure of the Big Hill fault dies to the north, but a north-trending syncline in Mangapanian deposits is present along the northern extension of the fault (Cutten, personal communication, 1989). Recent scarps can be seen on aerial photographs and in the field along much of the length of the Big Hill fault. On the south side of Big Hill Stream, the fault slightly offsets a stream terrace of indeterminant age. At both localities where the Big Hill fault is exposed within the study area, the fault is high angle. At the crossing of Big Hill Stream (Figure 2), striations trend 037° on the 120/63NE fault surface (Table 2) and are consistent with reverse offset along this leg of the fault.

Because of the striations at Big Hill Stream and the presence of WNW-ESE-trending folds between Big Hill and Ruahine faults (Figures 7 and 8), I infer that the more north-trending leg is predominantly a right-lateral slip fault. The WNW-ESE-trending folds within the Kaumatua and lower Ohara Mudstone (Figure 2 and Figure 10, cross section I) are consistent with a horizontal component of slip along the Big Hill fault. Assuming that the shortening recorded in these folds accommodates movement along the Big Hill fault, the total horizontal slip is estimated to be 0.5 km in a NE-SW direction. Vertical offset along the north-south-trending section is a minimum of 0.6 km (Figure 10, cross section A).

West of the southern end of the Big Hill block is the doubly-plunging Herricks anticline (Figure 7) (Kingma, 1958) and the adjacent Herricks syncline. The Herricks anticline and syncline form the most prominent features on the structural contour map (Figure 8). The folds are asymmetric, with the west limb of Herricks anticline dipping steeply, locally overturned and broken by the Thorn Flat fault (Figure 2 and Figure 10, cross sections B and C). I infer that the Thorn Flat fault is a high-angle reverse fault and dips approximately 50-60° to the east (Figure 10, cross sections B and C). Along part of the trace of the fault, a prominent lineation is visible on aerial photographs, and the lineation corresponds with a slight scarp that I observed in the field. The greatest cumulative horizontal shortening measured in the study area is along section line C of Figure 11 and is mainly due to 28% contractional strain accommodated by Herricks syncline and Thorn Flat fault.

The Matapuna fault (Figure 2 and Figure 10, cross sections F,G, and H) deforms sediments in the southern Ohara Depression. The fault is not exposed and is inferred from the steep dips in the Kaumatua Formation next to basement exposures (Figure 2). Small exposures of basement rocks also crop out at higher elevations where the only reasonable explanation is the existence of a fault. Though the Matapuna fault shows northwest-side-up vertical displacement, I infer the fault has a strike-slip component. Open folds in the Kaumatua Formation and the slight monocline in the Sentry Box Limestone in the vicinity of Sentry Box (Figures 2 and 7) are on strike with the northward extension of the Matapuna fault and I interpret that these folds are related to movement on the Matapuna fault. Contractional strain becomes slightly greater in the southern-most part of the Ohara Depression compared to the middle part because of basement uplift along the Matapuna fault and associated folding (Figure 11, line F versus line D).

Principal Stress Directions in the Ohara Depression Domain

The principal stress directions for the Ohara Depression domain were calculated using four megascale fault sites with slip indicators and two striated mesoscale fault sites (Figure 9) and the stress tensor analysis method of Angelier (1984). The maximum stress direction trends northeast and is subhorizontal. The intermediate and minimum stress axes are similar in magnitude (Table 5). The intermediate stress direction deviates 30-35° from the expected vertical orientation for a strike-slip fault. The deviation is probably related to the presence of dip-slip movement along the Ruahine and Mohaka faults, indicating that a transpressive strike-slip system exists within the Ohara Depression.

Deformation Related to the Wakarara Domain

The Wakarara fault and Wakarara monocline are the major structures east of the Mohaka fault (Figures 2 and 7), trending along the east front of the Wakarara Range. The bulk of the shortening occurring in the contractional Wakarara domain is accommodated along these two structures (Figures 7 and 8). The Wakarara monocline is locally over-

TABLE 5. Summary of stress tensor analysis.

Data Set	Cohesion[1]	No. of faults used	Orientation[2]						Ratio
			σ_1		σ_2		σ_3		σ_2/σ_3
			T	P	T	P	T	P	
Complete	87%	11	70	10	161	5	278	78	0.251
Ohara	100%	6	41	16	154	54	302	31	0.138
Wakarara	100%	5	230	25	139	0	48	65	0.181

[1] Cohesion indicates the percentage of striated faults used in the stress tensor analysis.

[2] For orientation of the principal stress axes:
T= trend of principal stress axis in degrees.
P= plunge of principal stress axis in degrees.

turned along the Wakarara Range front but dies out to the north (see cross sections H and A through F, Figure 10). The Wakarara monocline continues south along the eastern Wakarara Range front, across the east front of the Waipawa reentrant (Figure 7) (Raub, 1985), and along the east-stepping Ruahine Range front (Lillie, 1953) (Figure 7).

The Wakarara fault parallels and locally overthrusts the axis of the monocline along the eastern Wakarara Range front (Figure 7 and 8) (Grant-Taylor, 1978), but the surface trace disappears at the southern end of the Wakarara Range (Figure 7) (Raub, 1985). To the north, where the northern end of the Wakarara Range dips below the surface, the trace of the Wakarara fault dies out. The fault varies in dip from 66W to 82W in the exposures that I observed. Striations at several localities are consistent with reverse faulting with a small amount of dextral-slip (Table 2).

Basement rocks of the Wakarara Range have been uplifted along the fault and thrust over the Ohara Mudstone and younger units (Figures 2 and 8, and Figure 10, cross sections C through F and H). The formation of the Wakarara monocline is related to uplift of the Wakarara Range and movement along the Wakarara fault. Because of this relationship, I infer existence of the fault below the surface to the north by the presence of the Wakarara monocline (Figure 2 and Figure 10, cross sections A through C).

A relatively greater magnitude of shortening occurs on the Wakarara fault and monocline relative to areas farther west (see portions of lines D and F of Figure 11 that extend to the east side of the Wakarara Range). Line F (Figure 11) indicates the minimum amount of shortening because the original planation surface along the eastern front of the Wakarara Range has been eroded.

The Poporangi fault is a poorly-exposed fault that trends along a 4 km-long linear depression in the abandoned river terrace above Poporangi Stream southwest of Kereru Station and 1 km east of the Wakarara fault (Figure 2). Waghorn (1927) and Ongley (1943) reported that surface breaks occurred along the Poporangi fault during an earthquake in 1858. Several north-south- to northeast-soutwest-trending folds are present adjacent to the Poporangi fault (Figures 7 and 8). These folds are open though they can be locally abrupt. Some are associated with mesoscale thrust faults with throws of 0.1 to 1.5 m. At one locality close to the Wakarara fault, I observed an isoclinally folded tephra layer with a wave-length of 0.2 m and an amplitude of 1 m. Because of the folds adjacent to the Poporangi fault (Figures 7 and 8 and Figure 10, cross section D), I infer that it is dominantly a high-angle reverse fault related to the Wakarara fault.

East of the Wakarara monocline in the northeast part of the study area, there is a broad southeast warp in the upper Ohara Mudstone and overlying units (Figure 2 and 8) that I attribute to regional dextral shear.

Principal Stress Directions in the Wakarara Domain

Utilizing five striated fault measurements along and to the east of the Wakarara fault, I calculated the principle stress directions (Table 5 and Figure 9) for the Wakarara domain. The principal stress directions for the Wakarara domain show a subhorizontal, southwest-trending maximum stress direction, a horizontal intermediate stress direction and a near vertical minimum stress direction (Figure 9), which is consistent with both the predominantly high-angle reverse faulting along the east side of the eastern Wakarara Range and the uplift of the Wakarara Range.

Summary

The Ohara Depression-Wakarara Range region can be divided into two structural domains. The Ohara Depression domain is a dextral strike-slip belt bounded on the northwest and southeast by the Rauhine and Mohaka faults (Figure 7). The development of the Big Hill fault as a transfer fault between the Ruahine and Mohaka faults has resulted in the uplift of the Big Hill block and the formation of the Herricks anticline and syncline (Figure 8). To the south, the homoclinal structure of the Ohara Depression is disrupted by folding along part of the west side of the Mohaka fault and near the Ruahine fault by uplift of basement rocks along the Matapuna fault and folding of the overlying deposits (Figure 7). Horizontal contraction oblique to the strike-slip faults is greatest in the northern Ohara Depression domain as a result of the shortening recorded by the Herricks folds and the Thorn Flat fault (Figure 11, lines B and C).

The Wakarara domain is a contractional domain along the east front of the Wakarara Range, where shortening occurs by reverse faulting on the Wakarara fault and by the related folding recorded in the Wakarara monocline (Figures 8 and 11). Uplift of the Wakarara block occurs by dip-slip movement along the Wakarara fault and oblique-slip on the Mohaka fault. The magnitude of horizontal contraction measured along the east front of the Wakarara Range, as shown in Figure 11 (lines C through F and H), is only exceeded by the magnitude of contraction along the Herricks folds and the Thorn Flat fault.

The maximum compressive direction determined by the stress tensor analysis of striated faults is similar for both domains, differing mainly in the direction and amount of plunge (Table 5 and Figure 9). The calculated principal stress axes are consistent with a contractional domain with a slight amount of dextral slip along the Wakarara Range front and a strike-slip belt with some contraction transmitted obliquely to the orientation of the belt.

DISCUSSION

Tectonic Evolution of the Ohara Depression-Wakarara Range Region

In the Mangapanian (late Pliocene), uplift of the proto-Ruahine Range occurred, stripping sediments off of the planated surface of the Mesozoic rocks. Episodic influx of conglomerates, the presence of minor soft-sediment deformation and occasional intraformational unconformities in the Kaumatua Formation indicate that movement was occurring along the Ruahine fault. The Ohara block dropped down relative to the Ruahine block (Figures 12 and 13A) along the Ruahine fault as conglomerates, sandstones and mudstones of the Kaumatua Formation were deposited into the gradually subsiding lowlands to the east, though the waters remained relatively shallow.

By the early Nukumaruan (latest Pliocene) (Figures 12 and 13B), continued movement along the Ruahine fault had preserved the Kaumatua Formation to the east. The last pulse of coarse-clastic sediments from the west until the middle Nukumaruan was deposited within the Sentry Box Limestone, marking a period of submergence or subsidence of the Ruahine block and the Ohara block and a decrease in activity along the Ruahine fault. Waters within the Ohara Depression were shallower in the north, reflected by the unconformable contact between the Kaumatua Formation and the Sentry Box Limestone and the coarse clastic nature of the lower part of

Figure 12) Temporal distribution of tectonic activity of the structures inside and outside of the Ohara Depression. Solid line, geologic activity is certain in this time interval; dashed line, probable activity but data is insufficient; dashed and queried line, activity is uncertain due to lack of lithologic record.

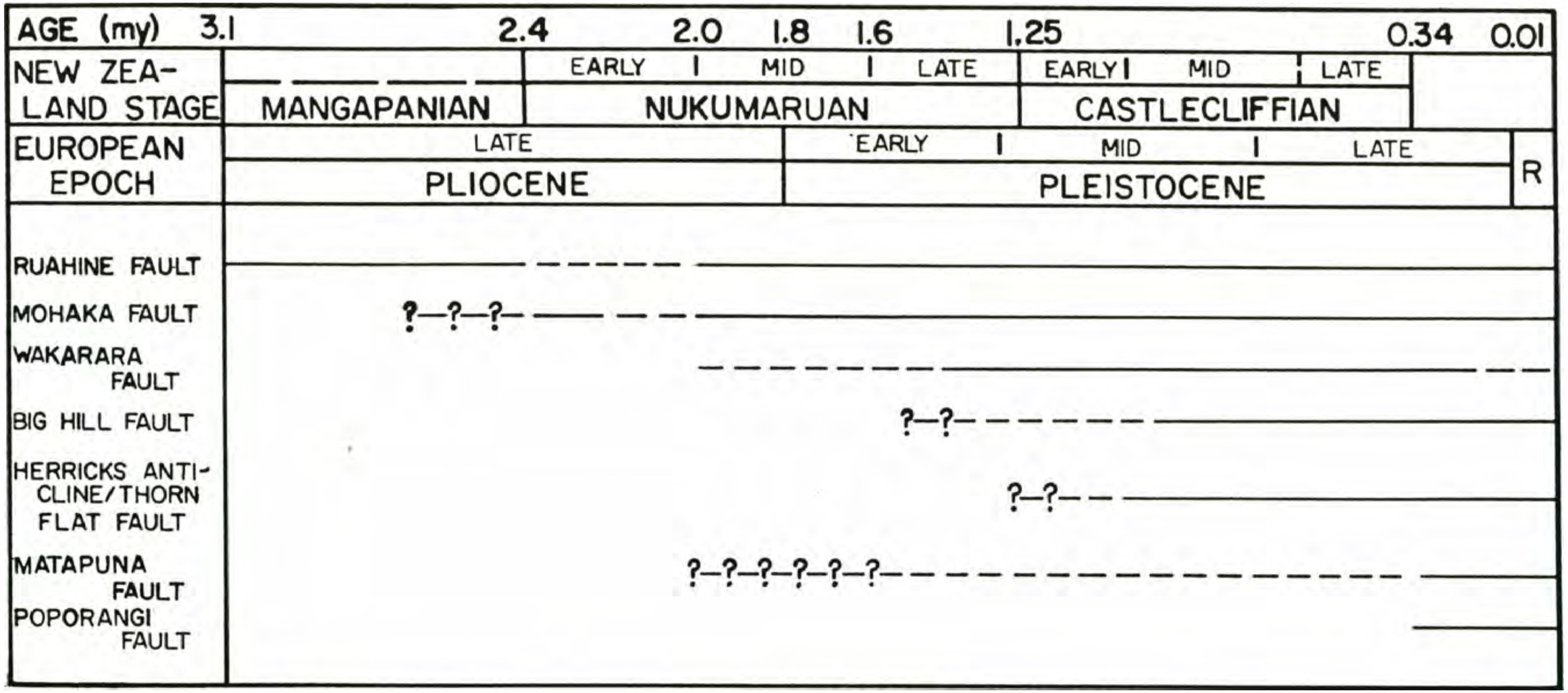
AGE (my) 3.1 2.4 2.0 1.8 1.6 1.25 0.34 0.01
NEW ZEALAND STAGE
MANGAPANIAN
EARLY MID LATE
NUKUMARUAN
EARLY MID LATE
CASTLECLIFFIAN
EUROPEAN EPOCH
LATE
PLIOCENE
EARLY MID LATE
PLEISTOCENE
R
RUAHINE FAULT
MOHAKA FAULT
WAKARARA FAULT
BIG HILL FAULT
HERRICKS ANTICLINE/THORN FLAT FAULT
MATAPUNA FAULT
POPORANGI FAULT

the Sentry Box Limestone. To the east, uplift of the Wakarara block along the middle segment of the Mohaka fault (Figure 13B) is recorded by the Mount Mary Limestone deposited on the planated Torlesse surface of the Wakarara block and off of the flanks of the Wakarara block, possibly into the Ohara Depression (Figure 2). Following the initial uplift of the Wakarara block, the Ohara Mudstone was deposited on the Ohara block and the Wakarara block, and probably on the Ruahine block as well.

During the mid to late Nukumaruan (early Pleistocene), partial emergence of the Ruahine block and the Wakarara block occurred again. Exposure of the Wakarara and Ruahine blocks is recorded by a sequence of shallowing and coarsening upward sediments beginning with the Kereru Limestone. The thick gravels near the base of the Okauawa Formation in the lower Ohara Stream (Figure 6) (McKay, 1877; Kingma, 1958) are correlated with the Kikowhero Gravels of Kingma (1971) and were probably derived from the northwest as the Ruahine Range began to emerge. The Ruahine fault probably continued to be active (Figure 12), dropping the Ohara block and preserving the Ohara Mudstone from erosion (Figure 13C). Partial emergence of the Wakarara Range occurred by reverse movement along the Wakarara fault and oblique-slip along the Mohaka fault (Figures 12 and 13C). I interpret that the gravels near the base of the Okauawa Formation along the east front of the Wakarara Range are derived from the Waka-

Figure 13) Sequential evolution diagram of the Ohara Depression-Wakarara Range region from Mangapanian (late Pliocene) to present. RF, Ruahine fault; MF, Mohaka fault; BHF, Big Hill fault; WAF, Wakarara fault; MPF, Matapuna fault; PF, Poporangi fault; TFF, Thorn Flat fault; HA, Herricks anticline; HS, Herricks syncline; BS, Balcony syncline; WAM, Wakarara monocline.

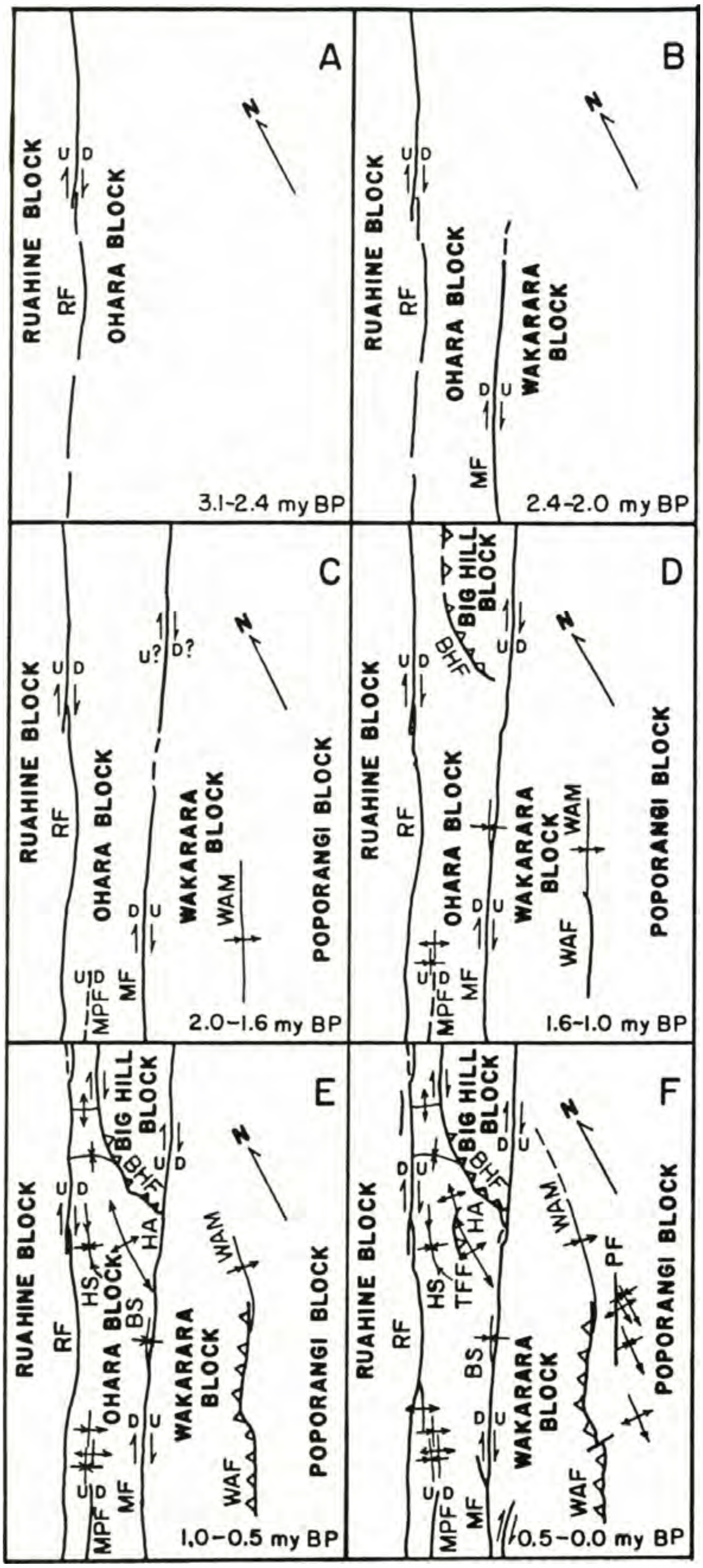
A
RUAHINE BLOCK
RF
U D
OHARA BLOCK
N
3.1-2.4 my BP
B
RUAHINE BLOCK
RF
U D
OHARA BLOCK
WAKARARA BLOCK
D U
MF
N
2.4-2.0 my BP
C
RUAHINE BLOCK
RF
U D
OHARA BLOCK
U? D?
WAKARARA BLOCK
WAM
D U
POPORANGI BLOCK
U D
MPF
MF
N
2.0-1.6 my BP
D
RUAHINE BLOCK
RF
U D
OHARA BLOCK
BIG HILL BLOCK
BHF
U D
WAKARARA BLOCK
WAM
D U
WAF
POPORANGI BLOCK
U D
MPF
MF
N
1.6-1.0 my BP
E
RUAHINE BLOCK
RF
U D
HS
OHARA BLOCK
BS
BIG HILL BLOCK
BHF
HA
U D
D U
WAKARARA BLOCK
WAM
WAF
POPORANGI BLOCK
U D
MPF
MF
N
1.0-0.5 my BP
F
RUAHINE BLOCK
RF
D U
HS
TFF
HA
BIG HILL BLOCK
BHF
D U
BS
WAKARARA BLOCK
WAM
PF
WAF
POPORANGI BLOCK
U D
MPF
MF
D U
N
0.5-0.0 my BP

rara Range as the Torlesse basement became exposed. The southern end of the Wakarara block emerged first as evidenced by the increasing abundance of coarse clastic sediments in a southerly direction along the east front of the Wakarara Range. The main uplift of the Wakarara Range did not occur until after the deposition of the Poutaki Pumiceous Formation. The main uplift is also probably contemporaneous with first motion on the Matapuna fault (Figures 12 and 13C) and folding of the Kaumatua Formation and the Sentry Box Limestone in the Sentry Box area (Figure 2).

By the latest Nukumaruan to Castlecliffian (mid-Pleistocene), the Ruahine block, the Wakarara block and to a lesser extent, the Ohara block, were subaerially exposed or were shallow, marginal seas. Pumiceous sands and gravels composed of Torlesse-derived sandstone and argillite clasts were deposited within the Ohara Depression (Raub, 1985) and to the east. The Big Hill fault began to develop (Figure 12), possibly as a reverse fault (Figure 13D). The southeast side of the northern segment of the Mohaka fault was dropped relative to the Big Hill block which was uplifted (Figure 13D-F). The Wakarara fault and monocline propagated northwards as the Wakarara block continued to uplift (Figure 13D). Uplift of the Wakarara block along the Mohaka fault is recorded within the Ohara block by folding of the Ohara Mudstone and the Kereru Limestone into the Balcony syncline (Figure 12 and 13D).

In mid- to late Castlecliffian (mid- to late Pleistocene), rapid uplift of the Ruahine and Wakarara Ranges occurred. The Big Hill fault probably began to transfer motion from the Ruahine fault to the Mohaka fault, forming the WNW-ESE-trending folds between the Ruahine Range and Big Hill (Figures 7 and 13E). As the Big Hill block continued to uplift and move south along the Big Hill fault, the Herricks anticline and syncline began to develop (Figures 12 and 13E). During the middle to late Castlecliffian, the greatest uplift took place along the Wakarara fault as recorded by the thick sequence of gravels of the Salisbury gravel lithofacies. Folding of the basal Salisbury gravel lithofacies also indicates that folding and faulting occurred after, if not during, deposition. Tephras deposited as ignimbrites at the base of the Salisbury gravel lithofacies to the east of the Wakarara Range indicate that topography was still fairly low at this time. There is no record of deposition within the Ohara Depression for the late Castlecliffian.

From the late Castlecliffian (late Pleistocene) to present (Figure 13F), the Wakarara monocline propagated farther north and uplift continued along the Wakarara fault. Dextral faulting began along the Poporangi fault, leading to the north-south trending folds in the Poporangi Stream area (Figure 13F). Movement continued along the Ruahine and Mohaka faults (Figure 12), but the southeast side was upthrown on both faults during the latest movement (Figure 13F). Folds within the Ohara Depression continued to develop, while the Matapuna fault and the Thorn Flat fault propagated upward and were exposed by erosion of the Plio-Pleistocene cover. The southern segment of the Mohaka fault was active at least by this time, as it doesn't appreciably deform the Mesozoic-Plio-Pleistocene contact at the southern end of the Wakarara Range (Raub, 1985). The dissection and erosion of river gravels and older marine deposits occurred inside and outside of the Ohara Depression.

Strain Partitioning of the Ohara/Wakarara Region

The style of uplift of basement blocks and the type of folding and faulting of sediments deposited on the blocks reflect a partitioning of strain. I will review the partitioning of strain, going westward across the Ohara/Wakarara area.

East of the Wakarara monocline and fault, the folds depicted in Figure 8 adjacent to the Poporangi fault are suggestive of contraction similar and perhaps related to contraction along the Wakarara fault and monocline. A southeast-dipping warp along the Ohara Stream east of the Wakarara monocline (Figures 2 and 8) may result from regional dextral shear.

Along the eastern front of the Wakarara Range, the dominant strain is east-west to northeast-southwest shortening (Figures 7, 8, 9 and 11). The shortening includes a small amount of dextral shear indicated by the southwest-plunging striae on the Wakarara fault (Table 2; Figure 9). Horizontal contraction along lines trending S60E is greatest east of the Wakarara Range (lines D and F, Figure 11), except for the large amount of shortening shown in line C of Figure 11. Extensional strain is occurring in a predominantly vertical direction (Figure 9) and is expressed by the uplift of the Wakarara Range.

West of the Wakarara Range, the two bounding faults of the Ohara Depression (the Ruahine and Mohaka faults) have accommodated translational strain. Striae on these dominantly strike-slip faults none-the-less have a vertical component of offset (Table 2; Figure 9). Although net uplift of the Ruahine Range is greater than the uplift of the Wakarara Range, the net vertical slip along the Mohaka fault is greater than the vertical slip along the Ruahine fault (Tables 3 and 4; Figure 10, cross sections D through H). Most of the Ohara Depression therefore dips homoclinally to the southeast.

Shortening has also occurred within the Ohara Depression, reflected in the Big Hill fault, Herricks anticline and syncline and the Thorn Flat fault in the north (Figure 10, cross sections B and C), by the Balcony syncline along the Mohaka fault (Figure 10, cross section D) and by the Matapuna fault and the associated folds in the Sentry Box area near the Ruahine fault (Figure 10, cross sections F, G and H).

The Big Hill fault presently transfers motion from the Ruahine fault to the Mohaka fault (Figure 7). The Big Hill fault may have developed as a transfer fault or it may have developed as a north-south-trending reverse fault (Figure 13D). The latter model is consistent with a component of contraction across the Mohaka fault in the latest Nukumaruan to Castlecliffian (early to mid-Pleistocene) and is consistent with the presence of folded but unfaulted Pliocene strata at the northern terminus of the Big Hill fault (H.N.C. Cutten, personal communication, 1989). The Big Hill block is tilted to the east (Figure 9) and vertical slip is as great or greater than horizontal slip along the Big Hill fault, so that the fault probably initially formed as a reverse fault.

The greatest shortening measured perpendicular to the main fault belt within the Ohara Depression is along line C of Figure 11. The shortening corresponds with Herricks syncline and slip along the Thorn Flat fault. Shortening along the Wakarara fault and monocline tapers off to the north (Figure 11) and uplift of the Wakarara block is much less, so that the contraction is possibly transmitted across the Mohaka fault north of the northern terminus of the Wakarara block. However, the transfer of motion from the Ruahine fault to the Mohaka fault along the Big Hill fault has resulted in the southward movement of the Big Hill block, which impinges on the rocks to the south and is therefore the primary reason for the development of these structures.

Contraction in the southern part of the Ohara Depression is much lower than contraction observed farther north in the Ohara Depression and along the eastern front of the Wakarara Range (Figures 8 and 11). Therefore, I conclude that vertical movement along the Mohaka fault has not only preserved the Plio-Pleistocene sediments within the Ohara Depression (Figure 10 cross section D through H), but is also a partitioning boundary, with minimal contraction west of the fault and substantial contraction east of the fault along the east front of the Wakarara Range.

Temporal Constraints on Deformation and Relation to Australia-Pacific Plate Motions

Two main episodes of uplift are recorded in the Ohara Depression-Wakarara Range region. The first episode began in the Mangapanian (late Pliocene), with the uplift of the proto-Ruahine Range. During the early Nukumaruan (latest Pliocene), submergence of most of the region occurred, except for the short-spanned uplift and exposure of the Wakarara Range. By the middle to late Nukumaruan (early Pleistocene), uplift and exposure of Ruahine and Wakarara Ranges occurred again. Translational and contractional structures developed within the Ohara Depression and along the eastern Wakarara Range front. Rapid uplift of the Ruahine and Wakarara Ranges took place during the Castlecliffian (mid-Pleistocene), along with less rapid uplift of the Ohara Depression and the Poporangi block. After the Castlecliffian (mid-Pleistocene), uplift slowed. However, deformation in the Ohara Depression and Wakarara Range region has continued.

Overall, uplift of the forearc basin is consistent with an increase in convergence between the Australian and Pacific plates (Gordon et al., 1988) about 3.4 my BP (Harbert and Cox, 1989). At the time of this change (Mangapanian or late Pliocene), coast-perpendicular convergence increased from 28 km/my to 35 km/my (Elder, 1990). Coast-parallel movement of the Pacific plate along a trend of N30E relative to the Australian plate increased only slightly, from about 21 km/my to 25 km/my (Elder, 1990).

The uplift of the proto-Ruahine Range in the Mangapanian (late Pliocene) follows the change in plate motion by about 0.3 my. The beginning of the next episode of uplift of the Ohara/Wakarara forearc area followed the change in plate motion by about 1.4 my with the maximum uplift occurring 1.6 my later, a delay perhaps due to other regional factors influencing uplift. The second period of uplift coincides with the main period of deformation within the Ohara Depression and along the east front of the Wakarara Range. Despite the delay, the blocks uplift and related faulting and folding are consistent with an increase in the rate of convergence between the Australian and Pacific plates and increase in the coast-perpendicular component of convergence at the latitude of Hawke Bay.

CONCLUSIONS

Uplift of basement blocks, the deformation of the Plio-Pleistocene sediments and patterns of sedimentation are related to the activity along the Ruahine, Mohaka Wakarara faults. Activity along the faults (Figure 12) can be constrained by structures associated with them, by the ages of the rock units deformed and by the sedimentary record preserved by subsequent uplift and faulting.

The megascale structures of the Ohara Depression and the Wakarara Range show that strain is partitioned into primarily contractional domain (Wakarara domain) and a primarily translational domain (Ohara Depression domain) but that in the Ohara Depressiona domain, contraction is present as well as translation. Stress tensor analysis of striated faults indicate different principal stress directions in the Ohara Depression domain versus the Wakarara domain. The Mohaka fault forms the boundary between the contractional domain to the east and the translational domain to the west.

Faults and folds in the Ohara Depression-Wakarara Range region are consistent with the east-to-west directed subduction of the Pacific plate beneath the northeast-trending eastern margin of North Island of New Zealand. The derived stress tensors are also consistent with present-day plate motions. An increase in the rate of convergence between the Australian and Pacific plates (Gordon et al., 1988) at about 3.4 my BP is followed by the main episode of uplift and development of deformation in the Ohara Depression-Wakarara Range region at approximately 1.8 to 0.4 my BP.

REFERENCES

Angelier, J. 1984: Tectonic analysis of fault slip data sets. *Journal of geophysical research 89B*: 5835-5848.

Beanland, S.; Berryman, K.R. 1987: Ruahine Fault Reconnaissance. *New Zealand Geological Survey report EDS109.*

Berryman, K.R. 1984: Late Quaternary tectonics of New Zealand. Pp 91-108: *in* An Introduction to the Recent Crustal Movements of New Zealand. Wellington, New Zealand. *Royal Society of New Zealand miscellaneous series* 7.

Beu, A.G. 1977: Transcurrent fault movements in central and southern Hawke's Bay since mid-Nukumaruan time. *Abstract, New Zealand Geological Survey Conference, Otaki, 10-14 October, 1977.*

Beu, A.G.; Grant-Taylor, T.L.; Hornibrook, N. de B. 1977: Nukumaruan records of the subantarctic scallop *Chlamys delicatula* and crab *Jacquinotia edwardsii* in central Hawke's Bay. *New Zealand journal of geology and geophysics 20*: 217-248.

Beu, A.G.; Grant-Taylor, T.L.; Hornibrook, N. de B. 1980: The Te Aute Limestone facies (Poverty Bay to northern Wairarapa). Wellington, New Zealand, Department of Scientific and Industrial Research. *New Zealand Geological Survey miscellaneous series map 13.*

Beu, A.G.; Browne, G.H.; Grant-Taylor, T.L. 1981: New *Chlamys delicatula* localities in the central North Island and uplift of the Ruahine Range. *New Zealand journal of geology and geophysics 24*: 127-132.

Beu, A.G.; Edwards, A.R.; Pillans, B.J. 1986: A review of New Zealand Pleistocene stratigraphy, with emphasis on marine rocks. *Proceedings of the first international colloquium on Quaternary stratigraphy of Asia and the Pacific, Osaka, 1986.*

Browne, G.H. 1986: Basement-cover relationships and tectonic significance of Mt. Miroroa, western Hawke Bay. *Journal of the Royal Society of New Zealand 4*: 381-402.

Cashman, S.M.; Kelsey, H.M. 1990: Forearc uplift and extension, southern Hawke's Bay, New Zealand: Mid-Pleistocene to present. *Tectonics 9*: 23-44.

Clark, C.L. 1976: Faunas, environments, and structural implications of Nukumaruan mudstone beds of the Ruataniwha Basin, Hawke's Bay. Unpublished M.Sc. thesis, lodged in the library, Univeristy of Auckland, Auckland, New Zealand.

Cutten, H.N.C.; Beanland, S.; Berryman, K.R. 1988: The Rangiora Fault, an active structure in Hawke's Bay. *New Zealand Geological Survey record 35*: 65-72.

Davey, F.J.; Hampton, M.; Childs, J.; Fisher, M.A.; Lewis, K.; Pettinga, J.R. 1986: Structure of a growing accretionary prism, Hikurangi margin, New Zealand. *Geology 14*: 663-666.

Dunham, R.J. 1962: Classification of carbonate rocks according to depositional texture. Pp. 108-121 *in*: Ham, W.E. *ed.* Classification of carbonate rocks. *American Association of Petroleum Geologists memoir 1.*

Edwards, A.R. 1985: A new integrated stratigraphy model for the late Neogene of New Zealand. Hornibrook Symposium, Extended Abstracts, *New Zealand Geological Survey record 9*, 41-43.

Edwards, A.R. 1987: An integrated biostratigraphy, magnetostratigraphy and oxygen isotope stratigraphy for the late Neogene of New Zealand. *New Zealand Geological Survey record 23*, 80 pp.

Elder, D. 1990: Forearc structures as a response to a Pliocene change in Pacific plate motion, North Island, New Zealand. Unpublished report, Western Washington University, 7 pp.

Folk, R.L.; Andrews, P.B.; Lewis, D.W. 1970: Detrital sedimentary rock classification and nomenclature for use in New Zealand. *New Zealand journal of geology and geophysics 13:* 937-968.

Gordon, R.G.; Demets, C.; Argus, D.F.; Stein, S. 1988: Current plate motions. AGU fall meeting, San Francisco, 6-11 December, 1988, *EOS, Transactions of the American Geophysical Union 69*, 1416.

Grant-Taylor, T.L. 1978: The geology and structure of the Ruataniwha Plains. Pp. 31-51 *in*: Speden, I. *ed.* Geology and erosion in the Ruahine Range. *New Zealand Geological Survey report G20.*

Grindley, G.W. 1960: Sheet 8-Taupo. Geological map of New Zealand, 1:250 000. Wellington, New Zealand, Department of Scientific and Industrial Research.

Harbert, W.; Cox, A. 1989: Late Neogene motion of the Pacific plate. *Journal of geophysical research 94B*: 3052-3064.

Hull, A.G. 1983: Trenching of the Mohaka Fault near Hautapu River, Hawke's Bay, 3-6 May 1983. Unpublished New Zealand Geological Survey report, file 831/26.

Hull, A.G. 1985: Holocene displacements at the Mohaka Fault, Northern Hawke's Bay. *Abstract, Geological Society of New Zealand Christchurch Conference, 9-13 December, 1985.*

Kingma, J.T. 1958: Geology of the Wakarara Range, central Hawke's Bay. *New Zealand journal of geology and geophysics 1*: 76-91.

Kingma, J.T. 1962: Sheet 11-Dannevirke. Geological map of New Zealand, 1:250 000. Wellington, New Zealand, Department of Scientific and Industrial Research.

Kingma, J.T. 1971: Geology of the Te Aute subdivision. *New Zealand Geological Survey bulletin 70.*

Le Pichon, X. 1968: Sea-floor spreading and continental drift. *Journal of geophysical research 73*: 3661-3697.

Lewis, K.B. 1980: Quaternary sedimentation on the Hikurangi oblique-subduction and transform margin, New Zealand. Pp. 171-189 *in*: Ballance, P.F.; Reading, H.G. *eds.* Sedimentation on Oblique-slip Mobile Zones. *Special publication of the International Association of Sedimentologists 4.*

McKay, A. 1877: Report on the country between Masterton and Napier. *Geological Survey reports of geological explorations 1876-7 10*: 67-94.

Ongley, 1943: Wairarapa Earthquake of 24th June 1942 with mapping showing surface traces of faults recently active. *New Zealand journal of science and technology 25*, 67-78.

Raub, M.L. 1985: The neotectonic evolution of the Wakarara area, southern Hawke's Bay, New Zealand. Unpublished M.Sc. thesis, lodged in the library, University of Auckland, Auckland, New Zealand.

Smale, D.; Houghton, B.F.; McKellar, I.C.; Mansergh, G.D.; Moore, P.R. 1978: Geology and erosion in the Ruahine Range: a reconnaissance study. Pp. 7-30 *in*: Speden, I. *ed.* Geology and erosion in the Ruahine Range. *New Zealand Geological Survey report G20.*

Speden, I.G. 1976: Fossil localities in Torlesse rocks of the North Island, New Zealand. *Journal of the Royal Society of New Zealand 6*: 73-91.

Sporli, K.B.; Bell, A.B. 1976, Torlesse melange and coherent sequences, eastern Ruahine Range, North Island, New Zealand. *New Zealand journal of geology and geophysics 19*, 427-447.

Stoneley, R.; Russel, W.A.C.; Haw, D. 1958: Waikaremoana-Wakarara Mountain front reconnaissance GR 4&5. BP-Shell and Todd Petroleum Development Ltd: New Zealand Geological Survey unpublished open-file petroleum report no. 307.

Te Punga, M.T. 1978: Upper Jurassic fossils from the Ruahine Range. *New Zealand journal of geology and geophysics 21*: 773-774.

Waghorn, R.J. 1927: "Earthquake rents" as evidence of recent surface faulting in Hawke's Bay. *New Zealand journal of science and technology 9*: 22-26.

Walcott, R.I. 1978: Geodetic strains and large earthquakes in the axial tectonic belt of North Island, New Zealand. *Journal of geophysical research 83B*: 4419-4429.

APPENDIX I.

TABLE OF FOSSIL SAMPLE LOCALITIES, AGE, ENVIRONMENT AND LITHOLOGIC UNIT FROM THE KERERU (U21), NAPIER (V21) AND WAIPAWA (V22) NZMS 260 MAPS.

NZMS 260- New Zealand Map Series 260, 1:50 000 scale topographic maps.

NZGS- New Zealand Geological Survey.

NZMG- New Zealand Map Grid. Example:

U21/078680,

U21 represents the NZMS 260 sheet to refer to;

078 is the easting in kilometers and tenths of kilometers: 7.8 km;

680 is the northing in kilometers and tenths of kilometers: 68.0 km.

Lithologic Units are represented by:

Tpto- Te Onepu Limestone

Tpkm- Kaumatua Formation

Tpsb- Sentry Box Limestone

TQoh- Ohara Mudstone

Qmk- Makaretu Clay

Qmr- Mason Ridge Limestone

Qmr(mst)- mudstone interval in the Mason Ridge Limestone

Qke- Kereru Limestone

Qok- Okauawa Mudstone

Qpu- Poutaki Pumiceous Formation

Ages are given in New Zealand ages:

nd- no age-diagnostic fossils present;

Wo- Opoitian (early Pliocene);

Wm- Mangapanian (mid- to late Pliocene);

Wn- Nukumaruan (late Pliocene to early Pleistocene);

Wc- Castlecliffian (mid-Pleistocene);

A query before an age indicates uncertainty in that age assignment. Example:

Wn-?Wc indicates certain age of Wn but range into Wc is uncertain.

A query after the age assignment indicates uncertainty in the whole range of the age assignment. Example:

Wo-Wm? indicates uncertain range from Wo to Wm, whereas Wo-Wm is certain.

TABLE OF FOSSIL SAMPLE LOCALITIES, AGE, ENVIRONMENT AND LITHOLOGIC UNIT FROM THE KERERU (U21), NAPIER (V21) AND WAIPAWA (V22) NZMS 260 MAPS.

FOSSIL RECORD #	NZGS SPECIMEN #	NZMG	LITHOLOGIC UNIT	AGE	ENVIRONMENT
U21/f36	F27048	U21/954723	Tpkm	Wo-Wm?	Inner- to mid-shelf; low energy, sheltered water
U21/f38	F27050	U21/985777	Tpkm	nd	Probably shelf
U21/f40	GS14506	U21/912631	Tpkm	Wm	Soft-bottom, shallow shelf
U21/f46	GS14513	U21/923669	Tpkm	Wm	Bathyal with reworked shallow marine fauna
U21/f49	GS14516	U21/926659	Tpkm	Wm	Near-shore, high energy
U21/f39	GS14505	U21/942685	Tpsb	early Wn	-------------
U21/f41	GS14507	U21/930634	Tpsb	early Wn	Mixed nearshore and outer shelf/upper bathyal
U21/f43	GS14509	U21/933661	Tpsb	early Wn	-------------
U21/f62	GS14611	U21/933646	Tpsb	early Wn	Cold water fauna
U21/f8566	GS11781	U21/936665	TQoh	early Wn	Bathyal
U21/f32	F27047	U21/008683	TQoh	Wn-	Neritic water, shelf assemblage
U21/f37	F27049	U21/997705	TQoh	?Wm-Wn	Neritic water, shelf assemblage

FOSSIL RECORD #	NZGS SPECIMEN #	NZMG	LITHOLOGIC UNIT	AGE	ENVIRONMENT
U21/f44	GS14511	U21/008683	TQoh	early Wn	Mixed fauna of inner shelf and upper bathyal
U21/f47	GS14514	U21/997705	TQoh	--------	Taxa living on hard substrate
U21/f48	GS14515	U21/939664	TQoh	Wn?	Soft-bottom, 5-200m
U21/f52	-------	U21/940664	TQoh	nd	Soft-bottom, shallow marine, c. 10-20 m
U21/f53	-------	U21/941663	TQoh	nd	Soft-bottom, shallow marine
U21/f54	-------	U21/942663	TQoh	Wn?	Inner- to mid-shelf, soft-bottom
U21/f55	-------	U21/942662	TQoh	Wn?	Soft-bottom, shallow marine
U21/f56	-------	U21/943662	TQoh	Wn?	Soft-bottom, depth c. 40-60 m
U21/f57	-------	U21/944661	TQoh	Wm-Wn	Soft-bottom, shallow marine
U21/f58	-------	U21/938664	TQoh	Wn?	Soft-bottom, shallow marine
U21/f45	GS14512	U21/f45	Qke	mid- to late Wn	------------

FOSSIL RECORD #	NZGS SPECIMEN #	NZMG	LITHOLOGIC UNIT	AGE	ENVIRONMENT
U21/f42	GS14508	U21/032700	Qok	mid- to late Wn	Shallow, mid- to inner-shelf, soft-bottom
U21/f50	GS14539	U21/021676	Qok	Wn-?Wc	Soft-bottom, shallow marine
U21/f51	GS14540	U21/023677	Qok	Wn	Very shallow marine water, protected bay
U21/f60	GS14582	U21/050668	Qok	mid- to late Wn	Shallow marine, protected bay
U21/f61	GS14583	U21/078680	Qok	mid- to late Wn	Shallow marine, current swept
U21/f59	-------	U21/?	----	nd	Shelf depth
V21/f97	GS14584	V21/110655	Qpu	Wn	Estuary or nearly so
V21/f96	GS14584	V21/139646	Qmr	mid- to late Wn	Very shallow marine, c. 3-5m, in wave zone of low energy (protected) beach
V21/f98	GS14586	V21/146651	Qmr (mst)	mid- to late Wn	Inner- to mid-shelf
V21/f99	GS14610	V21/147620	Qmr (mst)	mid- to late Wn	Inner- to mid-shelf, quiet deposition, soft substrate

FOSSIL RECORD #	NZGS SPECIMEN #	NZMG	LITHOLOGIC UNIT	AGE	ENVIRONMENT
V21/f100	GS14609	V21/204605	Qmk?	mid-Wn	Shallow marine, inner shelf
V22/f141	GS14581	V22/150594	Qmk	mid-Wn	----------------------
V22/f142	F27343	V22/133432	Qmk	Wn	Shelf
V22/f143	F27344	V22/303599	Tpto?	Wm-Wn, prob. Wn	Shelf
V22/f156	F27352	V22/119405	Qmk	Wn	Shelf

APPENDIX II.

LOCATION AND STRATIGRAPHIC POSITION OF TEPHRA SAMPLES FROM THE HAWKE'S BAY DISTRICT

Several tephra layers and ignimbrites were found during my mapping of portions of the Kereru (U21), Napier (V21) and Waipawa (V22) NZMS 260 maps. The following table gives a listing of tephra/ignimbrite deposits which were collected during January 1988-June 1988 and November and December of 1988. Listed are the sample identification, a brief verbal description of the location, the inferred or known stratigraphic location of the deposit and the New Zealand Map Grid (NZMG) coordinates for the site location (see Appendix I for an explanation of the NZMG).

TABLE OF THE LOCATION AND STRATIGRAPHIC POSITION OF TEPHRA SAMPLES FROM THE HAWKE'S BAY DISTRICT

SAMPLE #	SAMPLE LOCATION	INFERRED STRATIGRAPHIC POSITION	NZMG
17K3	On farm track on Mananui Station	Base of Salisbury gravel lithofacies; same as 30K11?	V22/133460
30K11	SE fork of S fork of Yarrow Str	Base of Salisbury gravel lithofacies	V21/122620
29K2	Highway 50, Hawke's Bay	Base of Salisbury gravel lithofacies; same as 30K11?	U22/084569
13L2a	Yarrow Stream W of Ben Lomond	Base of Salisbury gravel lithofacies; same as 30K11?	V21/103620
13L2c	Yarrow Stream SW of Ben Lomond	Base of Salisbury gravel lithofacies; same as 30K11?	V21/102617
5L10	Upper Okauawa Stream	Base of Salisbury gravel lithofacies; same as 30K11?	U21/085648
25L3c	Unnamed stream S of Eaton	Base of Salisbury gravel lithofacies?; same as 30K11?	U21/004631
25L4	Unnamed stream S of Eaton, at chute	Base of Salisbury gravel lithofacies?; same as 30K11?	U21/990629
12L5	Poutaki Stream at top of bluff	Base of Salisbury gravel lithofacies?; same as 30K11?	U21/997646
27L1A	Tributary of Poporangi Str, near Waitangi	Base of Salisbury gravel lithofacies?; same as 30K11?	U21/023682

SAMPLE #	SAMPLE LOCATION	INFERRED STRATIGRAPHIC POSITION	NZMG
13MA3	Unnamed stream S. of Eaton	Unknown. Salisbury gravel lithofacies?	U21/988629
WS22	Waitangi Stream, near limestone outcrop	32m above base of Kereru Limestone. Okauawa Formation.	U21/017690
13MA2	Tributary of Poporangi Stream S. of Eaton	Same as WS22. Okauawa Formation.	U21/987628
28K3	Ngaruroro River, west of Boar's Leap	11m above 15m thk. cgl bed;Same as WS22? Okauawa Formation.	V21/102750
24JA1	Ohara Stream at bend north of Big Hill Rd.	7m above lower cgl bed; Same as WS22? Okauawa Formation.	U21/046728
14MA6	Upper Poporangi Stream in limestone beds	Approx. 2m below top of Kereru Limestone	U21/979601
WS17	Lower ash from Waitangi Stream	130m below base of Kereru Limestone Ohara Mudstone.	U21/015689
3F3	Ohara Stream below confluence of Poporangi	130-160m below Kereru Limestone; same as WS17? Ohara Mudstone.	U21/053743
12A4	Poutaki Stream at Wakarara fault	Approx. 100m below base of Kereru Limestone. Ohara Mudstone.	U21/989644

SAMPLE #	SAMPLE LOCATION	INFERRED STRATIGRAPHIC POSITION	NZMG
20MR3	Ohara Stream near Tarapeke Stream	Approx. 60m below Kereru Limestone; correlative with WS17? Ohara Mudstone.	U21/958671
25F5	Mathew's Stream, north of Glendale Station.	Same as JUS9?? or 20MR3?? Ohara Mudstone.	U21/964696
JUS9	Jumped Up Stream east of Mangleton Rd.	50m above top of Sentry Box Limestone Ohara Mudstone.	U21/937664
26MR6	Sentry Box Stream east of Mangleton Rd.	Same as JUS9. Ohara Mudstone.	U21/936660
7A3	Ohara Stream near Kaumatua Stream	Same as JUS9? Ohara Mudstone.	U21/937648
11L11	Te Onepu Rd.	At base of lowest Mason Ridge Limestone; lower Wn. Same as JUS9? Makaretu Clay.	V22/178508
18K2	Washpool Ridge in calcarenite	Mason Ridge bed #1; Same as 11L11??	V21/275628
24MR1	Mathew's Stream upstream of old access	Same as JUS9??/Reworked junk? Ohara Mudstone.	U21/956697
21F3C	Kaumatua Stream	Below barnacle-rich and oyster-rich shell bed. Probably reworked. Kaumatua Formation.	U21/927644
17MA1	Western slope of Big Hill in gully	Unknown, poss. same as 21F3C? Kaumatua Formation; probably Wm.	U21/992779

APPENDIX III.

GLASS CHEMISTRIES OF TEPHRA SAMPLES FROM THE OHARA DEPRESSION-WAKARARA RANGE REGION.

The following is a table of glass chemistry analysis of some of the tephra samples collected from my thesis study area. Analysis was done using an electron microprobe by P. Shane and Brad Pillans of Victoria University of Wellington, New Zealand. All values are given in weight percent oxides. N/A indicates that the data were not available for that particular oxide. Sample identification is the same as that used in Appendix II.

TABLE OF GLASS CHEMISTRIES OF TEPHRA SAMPLES FROM THE OHARA DEPRESSION-WAKARARA RANGE REGION.

	WS17	**WS22**	**13MA2**	**13MA3**	**7A3**
SiO_2	75.99(0.51)	76.32(0.51)	76.91(0.31)	75.83(0.90)	76.15(0.45)
Al_2O_3	13.00(0.14)	13.03(0.16)	12.77(0.16)	13.01(0.34)	12.73(0.16)
TiO_2	0.10(0.04)	0.12(0.01)	0.14(0.04)	0.10(0.04)	0.18(0.08)
FeO	1.64(0.15)	1.13(0.09)	1.07(0.07)	1.56(0.26)	1.36(0.21)
MgO	0.09(0.02)	0.11(0.02)	0.14(0.03)	0.06(0.02)	0.18(0.06)
CaO	1.15(0.10)	1.07(0.11)	1.00(0.09)	0.78(0.15)	1.30(0.28)
Na_2O	4.11(0.24)	3.79(0.10)	3.62(0.18)	4.35(0.25)	3.77(0.23)
K_2O	3.71(0.17)	4.21(0.21)	4.24(0.24)	4.09(0.23)	4.08(0.50)
Cl	0.21(0.02)	0.23(0.02)	0.11(0.02)	0.22(0.03)	0.25(0.05)
H_2O	7.13(1.47)	7.78(1.51)	7.01(1.65)	6.65(0.76)	8.62(2.33)

	24JA1	**25F5**	**14MA6**	**17MA1**
SiO_2	77.45(0.55)	75.82(0.47)	77.84(0.43)	76.22(0.89)
Al_2O_3	12.42(0.19)	13.00(0.18)	12.14(0.25)	13.28(0.32)
TiO_2	0.18(0.08)	0.23(0.09)	0.19(0.05)	0.19(0.05)
FeO	1.12(0.14)	1.73(0.22)	1.24(0.15)	1.43(0.19)
MgO	0.11(0.03)	0.23(0.06)	0.17(0.06)	0.22(0.05)
CaO	1.05(0.13)	1.60(0.08)	1.25(0.27)	1.36(0.05)
Na_2O	3.59(0.17)	3.86(0.35)	3.47(0.26)	4.40(0.27)
K_2O	3.93(0.25)	3.33(0.21)	3.57(0.76)	2.82(0.16)
Cl	0.21(0.02)	0.23(0.02)	0.11(0.02)	0.22(0.03)
H_2O	N/A	N/A	N/A	N/A

APPENDIX IV.

ORIENTATION OF MEGA- AND MESOSCALE FAULTS WITH SLIP INDICATORS IN THE OHARA DEPRESSION-WAKARARA RANGE REGION.

The following table is a list of sites where I observed striations on fault surfaces or slip directions were determined using the off-set of geomorphic features and projecting the horizontal-to-vertical slip-ratio onto the fault plane. A verbal description of the location, description of the fault, a site identification and a description of the lineation are included along with the orientation of the fault surface, the orientation of the lineation and the sense of slip of the fault.

TABLE OF THE ORIENTATION OF MEGA- AND MESOSCALE FAULTS WITH SLIP INDICATORS IN THE OHARA DEPRESSION-WAKARARA RANGE REGION.

FAULT	SITE ID	FAULT ORIENTATION[1]		LINEATION ORIENTATION[2]			DESCRIPTION OF LINEATION
		S	D	T	P	S	
Ruahine (southern segment)	22MR1A	32	90	32	25	(D)	gouge w/striae
Big Hill	7MY1	120	63NE	37	60	(R)	gouge w/striae
Mohaka (mid-southern segment)	28MR1	29	89SE	30	47	(D)	gouge w/striae
Mohaka (mid-northern segment)	31JA2	120	40NW	24	6	(D)	offset ridges
Wakarara	12A4	18	79NW	211	58	(R)	gouge w/striae
Wakarara	12A4	177	59NW	205	39	(R)	gouge w/striae
Wakarara	12A4	177	59NW	242	56	(R)	gouge w/striae
Wakarara	13MA1	170	64NW	241	63	(R)	gouge w/striae
Mesofault near Ruahine fault	26MR6	102	82SW	104	08	(S)	gouge w/striae
Mesofault near Kaumatua Str.	26L1	78	82NW	073	24	(S)	gouge w/striae
Mesofault east of Wakarara flt.	3F4	140	25SW	270	21	(R)	gouge w/striae

[1] S, strike; D, dip.

[2] T, trend; P, plunge; S, fault sense: D, dextral; S, sinistral; R, reverse.

APPENDIX V.

LISTING OF THE ANGELIER-STYLE FILES OF THE STRIATED FAULTS IN THE OHARA DEPRESSION AND WAKARARA DOMAINS USED FOR PERFORMING STRESS TENSOR ANALYSIS IN THE OHARA DEPRESSION-WAKARARA RANGE REGION.

STRSLP.ANG: (for analyzing the Ohara Depression Domain)

```
02 60188   1-37750 176250 23 1 6                              STRSLP    1
01CFERDMAN
01WESTERN HAWKE'S BAY, NEWZEALAND
01PLIO-PLEISTOCENE MARINE SEDIMENTS
01STRIKE-SLIP BELT IN OBLIQUE CONVERGENT MARGIN
14 30632731 7 7 700      0  00BHF;OM-TSG cntct  CI 120 63E 87E7MY1      1
24348823401 7 7 700      0  00KF;Sinferred;     PS  78 82N 20E26L1      3
12300401721 7 7 700      0  00MF at Balcony;OM- CD  30 40W  2431JA2     4
13119892271 7 7 700      0  00MF;TSG-OM cntct;  CD  29 89E 47N28MR1     5
1119282  81 7 7 700      0  00KF;late;CUTS#10,1 CS 102 82S  8E11MY1     6
13122892051 7 7 700      0  00RF;gouge w/striae CD  32 90* 25N22MR1A    7
03R2DS05214.0  .0304.0  .0360.090.0 .00121.5 83.CPS19   6.  6STRSLP     1
03R2DT05215.0  .0305.0  .0360.090.0 .00121.8 83.CPS19   6.  6STRSLP     2
03R4DS05 40.214.7151.153.5300.632.5 .126 7.6100.CPS19   6.  6STRSLP     3
03R4DT05 40.414.8151.253.4300.632.6 .128 7.6100.CPS19   6.  6STRSLP     4
00*********************************************************STRSLP
09*****************************************************
```

THRUST.ANG: (for analyzing the Wakarara Domain)

```
02 60188   1-37750 176250 23 1 6                              THRUST    1
01CFERDMAN
01WESTERN HAWKE'S BAY, NEWZEALAND
01PLIO-PLEISTOCENE MARINE SEDIMENTS
01STRIKE-SLIP BELT IN OBLIQUE CONVERGENT MARGIN
14230253071 7 7 700      0  00OM;040/7E;EWAM    CI 140 25W 2703F4       2
13288792381 7 7 700      0  00WAF;TSG-OM cntct  CI  18 79W 58S12A4      8
13267592271 7 7 700      0  00WAF;TSG-OM cntct  CI 177 59W 47S12A4      9
13267592401 7 7 700      0  00WAF;TSG-OM cntct  CI 177 59W 60S12A4     10
13260642611 7 7 700      0  00WAF;TSG-OM cntct  CI 170 64W 81S13MA1    11
03INVD00246.8 4.2156.5 4.0 23.384.2 .28918.0100.CPS19   5.  5THRUST     1
03R2DT05 68.1  .0158.1  .0360.090.0 .50319.2100.CPS19   5.  5THRUST     2
03R2DS05 73.3  .0163.3  .0360.090.0 .12417.4100.CPS19   5.  5THRUST     3
03R4DT05229.224.9139.1  .3 48.565.1 .17010.6100.CPS19   5.  5THRUST     4
03R4DS05229.724.8139.5  .5 48.465.1 .18110.6100.CPS19   5.  5THRUST     5
00*********************************************************THRUST
09*****************************************************
```

APPENDIX VI.

RESULTS FROM THE STRESS TENSOR ANALYSIS PROGRAM OF ANGELIER

R2DS, R2DT, R4DS and R4DT are all different methods of analysis within Jacques Angelier's program TENSOR. The 'S' indicates a sine function was used for calculating the stress tensors, while a 'T' indicates a tangent function was used. The tangent function is quicker and usually yields values close to those obtained by utilizing a sine function for the calculation. The '2' apparently indicates that a simpler model for deformation is assumed in analyzing the data.

SIGMA 1: maximum compressive stress direction.

SIGMA 2: intermediate stress direction.

SIGMA 3: minimum compressive stress direction.

RAPPORT PHI: $\sigma_2-\sigma_3/\sigma_1-\sigma_3$

If ϕ=0.5, then the orientation of the axes is well-defined. If ϕ is close to 0.0, then the orientation of the axes for σ_2 and σ_3 are not well-constrained because they are similar in length. If ϕ is close to 1.0, then the orientation of the axes for σ_1 and σ_2 are not well-constrained because they are similar in length.

MESURE: the identification number given to the fault in the input file.

POIDS: the weight given to the fault for the analysis. 1.0 is full weight. Less than 1.0 indicates a lower importance or trust-worthiness of the data, as assigned by the user.

STR,T: the angle between the theoretical slip direction and the actual orientation of the lineation. One exclamation mark (!) to the right of this column indicates a questionable fit; two exclamation marks (!!) indicates a fault and lineation measurement which was rejected for the analysis (the angle between the actual and theoretical is greater than 45°).

COHESION: the percentage of fault/lineation pairs retained for the analysis.

Results from the Ohara Depression Domain:

```
**********************************************************************
* PROGRAMME TENSOR, VERSION R2DT 5  REFERENCE  5  J.ANGELIER,1975,1984 *
* SITE STRSLP     TYPES CPS  POND.1  CHRONOL.9****  NBR=  6  TOT=  6.0 *
**********************************************************************

                    AXE SIGMA 1      D= 216.      P=   0.
                    AXE SIGMA 2      D= 306.      P=   0.
                    AXE SIGMA 3      D= 360.      P=  90.
                    RAPPORT PHI=  .001  PSI=-1.543 RAD.

 MESURE  POIDS  SIGMA SIGMAN  TAU   RO  UPSILO  RMU    SIG,N      STR,T  45
     1.    1.0   1.61  1.19  1.08   .11   .24    .91    42.          6.
     3.    1.0   1.34   .28  1.31   .29   .50   4.60    78.         13.
     4.    1.0    .88  -.87   .17   .04   .70    .20    11.  ?      13.
     5.    1.0    .90  -.84   .31   .23   .69    .37    21.         47. !!
     6.    1.0   1.63  1.28  1.01   .44   .44    .79    38.         25.  !
     7.    1.0    .88  -.87   .18   .08   .71    .21    12.  ?      25.  !

 MESURE  POIDS  SIGMA SIGMAN  TAU   RO  UPSILO  RMU    SIG,N      STR,T  45
 MOYENNE   1.0   1.21   .03   .68   .20   .55   1.18    34.         21. 16.
 (COHESION 83.)
 ECART-TYPE       .33   .94   .47   .14   .17   1.55    23.         13.  8.

**********************************************************************
* PROGRAMME TENSOR, VERSION R2DS 5  REFERENCE  6  J.ANGELIER,1975,1984 *
* SITE STRSLP     TYPES CPS  POND.1  CHRONOL.9****  NBR=  6  TOT=  6.0 *
**********************************************************************

                    AXE SIGMA 1      D= 215.      P=   0.
                    AXE SIGMA 2      D= 305.      P=   0.
                    AXE SIGMA 3      D= 360.      P=  90.
                    RAPPORT PHI=  .001  PSI=-1.574 RAD.

 MESURE  POIDS  SIGMA SIGMAN  TAU   RO  UPSILO  RMU    SIG,N      STR,T  45
     1.    1.0   1.58  1.18  1.06   .08   .21    .90    42.          4.
     3.    1.0   1.33   .31  1.29   .28   .48   4.15    76.         13.
     4.    1.0    .87  -.85   .15   .03   .72    .18    10. ??      12.
     5.    1.0    .88  -.83   .28   .20   .71    .33    18.  ?      47. !!
     6.    1.0   1.61  1.28   .98   .43   .43    .76    37.         26.  !
     7.    1.0    .87  -.85   .14   .06   .74    .17    10. ??      25.  !

 MESURE  POIDS  SIGMA SIGMAN  TAU   RO  UPSILO  RMU    SIG,N      STR,T  45
 MOYENNE   1.0   1.19   .04   .65   .18   .55   1.08    32.         21. 16.
 (COHESION 83.)
 ECART-TYPE       .33   .94   .47   .14   .19   1.40    23.         14.  8.
```

```
***************************************************************************
* PROGRAMME TENSOR, VERSION R4DT 5  REFERENCE  3  J.ANGELIER,1975,1984 *
* SITE STRSLP     TYPES CPS  POND.1  CHRONOL.9****  NBR=  6  TOT=  6.0 *
***************************************************************************

                 AXE SIGMA 1      D=  42.      P=  16.
                 AXE SIGMA 2      D= 154.      P=  54.
                 AXE SIGMA 3      D= 302.      P=  32.
                 RAPPORT PHI=  .138  PSI=-1.407 RAD.

MESURE  POIDS  SIGMA SIGMAN  TAU   RO  UPSILO  RMU    SIG,N     STR,T  45
    1.    1.0   2.07    .85  1.89   .18  1.03  2.21     66.        5.
    3.    1.0   1.79   -.15  1.78   .12   .92 11.77     85.        4.
    4.    1.0   1.33   -.65  1.16   .05   .30  1.79     61.        2.
    5.    1.0   1.58 -1.32    .87   .22   .22   .66     33.       14.
    6.    1.0   2.42  1.68   1.74   .14   .88  1.04     46.        5.
    7.    1.0   1.55 -1.39    .69   .15   .25   .49     26.       13.

MESURE  POIDS  SIGMA SIGMAN  TAU   RO  UPSILO  RMU    SIG,N     STR,T  45
MOYENNE   1.0   1.79   -.16  1.35   .14   .60  2.99     53.        7.  7.
(COHESION100.)
ECART-TYPE       .36  1.12    .47   .05   .35  3.97     20.        5.  5.
```

```
***************************************************************************
* PROGRAMME TENSOR, VERSION R4DS 5  REFERENCE  4  J.ANGELIER,1975,1984 *
* SITE STRSLP     TYPES CPS  POND.1  CHRONOL.9****  NBR=  6  TOT=  6.0 *
***************************************************************************

                 AXE SIGMA 1      D=  41.      P=  16.
                 AXE SIGMA 2      D= 154.      P=  54.
                 AXE SIGMA 3      D= 302.      P=  31.
                 RAPPORT PHI=  .138  PSI=-1.413 RAD.

MESURE  POIDS  SIGMA SIGMAN  TAU   RO  UPSILO  RMU    SIG,N     STR,T  45
    1.    1.0   2.07    .85  1.89   .17  1.03  2.21     66.        5.
    3.    1.0   1.79   -.15  1.78   .12   .92 11.93     85.        4.
    4.    1.0   1.33   -.65  1.16   .04   .30  1.79     61.        2.
    5.    1.0   1.59 -1.33    .87   .22   .22   .65     33.       14.
    6.    1.0   2.42  1.68   1.74   .14   .88  1.03     46.        5.
    7.    1.0   1.55 -1.39    .68   .15   .25   .49     26.       13.

MESURE  POIDS  SIGMA SIGMAN  TAU   RO  UPSILO  RMU    SIG,N     STR,T  45
MOYENNE   1.0   1.79   -.16  1.35   .14   .60  3.02     53.        7.  7.
(COHESION100.)
ECART-TYPE       .36  1.12    .47   .05   .35  4.03     20.        5.  5.
```

Results from the Wakarara Domain:

```
***************************************************************************
* PROGRAMME TENSOR, VERSION R2DT 5  REFERENCE  5  J.ANGELIER,1975,1984 *
* SITE THRUST     TYPES CPS  POND.1  CHRONOL.9****  NBR=  5  TOT=  5.0 *
***************************************************************************

                    AXE SIGMA 1      D=  68.       P=   0.
                    AXE SIGMA 2      D= 158.       P=   0.
                    AXE SIGMA 3      D= 360.       P=  90.
                    RAPPORT PHI=  .503  PSI= -.655 RAD.

 MESURE  POIDS  SIGMA SIGMAN  TAU   RO  UPSILO  RMU   SIG,N     STR,T  45
     2.    1.0    .92  -.61   .68  .31    .41  1.12    48.        27.  !
     8.    1.0    .72   .49   .52  .23    .46  1.07    47.        26.  !
     9.    1.0    .89   .36   .81  .35    .38  2.24    66.        26.  !
    10.    1.0    .89   .36   .81  .18    .19  2.24    66.        13.
    11.    1.0    .91   .53   .73  .05    .15  1.37    54.         4.

 MESURE  POIDS  SIGMA SIGMAN  TAU   RO  UPSILO  RMU   SIG,N     STR,T  45
 MOYENNE   1.0    .86   .23   .71  .22    .32  1.61    56.        19. 19.
 (COHESION100.)
 ECART-TYPE       .07   .42   .11  .11    .12   .53     8.         9.  9.

***************************************************************************
* PROGRAMME TENSOR, VERSION R2DS 5  REFERENCE  6  J.ANGELIER,1975,1984 *
* SITE THRUST     TYPES CPS  POND.1  CHRONOL.9****  NBR=  5  TOT=  5.0 *
***************************************************************************

                    AXE SIGMA 1      D=  73.       P=   0.
                    AXE SIGMA 2      D= 163.       P=   0.
                    AXE SIGMA 3      D= 360.       P=  90.
                    RAPPORT PHI=  .124  PSI= -.202 RAD.

 MESURE  POIDS  SIGMA SIGMAN  TAU   RO  UPSILO  RMU   SIG,N     STR,T  45
     2.    1.0    .74  -.39   .63  .16    .30  1.62    58.        15.
     8.    1.0    .94   .56   .75  .48    .56  1.35    53.        40.  !
     9.    1.0    .99   .57   .80  .28    .30  1.40    54.        21.
    10.    1.0    .99   .57   .80  .11    .13  1.40    54.         8.
    11.    1.0   1.03   .75   .71  .05    .17   .94    43.         4.

 MESURE  POIDS  SIGMA SIGMAN  TAU   RO  UPSILO  RMU   SIG,N     STR,T  45
 MOYENNE   1.0    .94   .41   .74  .22    .29  1.34    53.        17. 17.
 (COHESION100.)
 ECART-TYPE       .10   .41   .06  .15    .15   .22     5.        12. 12.
```

```
*********************************************************************
* PROGRAMME TENSOR, VERSION R4DT 5  REFERENCE  7  J.ANGELIER,1975,1984 *
* SITE THRUST     TYPES CPS  POND.1  CHRONOL.9****  NBR=  5  TOT=  5.0 *
*********************************************************************

                     AXE SIGMA 1      D= 229.      P=  25.
                     AXE SIGMA 2      D= 139.      P=   0.
                     AXE SIGMA 3      D=  48.      P=  65.
                     RAPPORT PHI=  .170  PSI= -.791 RAD.

 MESURE  POIDS  SIGMA SIGMAN  TAU   RO  UPSILO  RMU   SIG,N     STR,T  45
    2.     1.0   1.77 -1.77   .01   .00   .85   .01     0. ??      2.
    8.     1.0   1.51  -.56  1.40   .34   .60  2.49    68.        14.
    9.     1.0   1.80  -.83  1.60   .49   .82  1.92    62.        18.
   10.     1.0   1.80  -.83  1.60   .13   .74  1.92    62.         5.
   11.     1.0   1.97  -.39  1.93   .50  1.11  4.90    78.        15.

 MESURE  POIDS  SIGMA SIGMAN  TAU   RO  UPSILO  RMU   SIG,N     STR,T  45
 MOYENNE   1.0   1.77  -.88  1.31   .29   .82  2.24    54.        11. 11.
 (COHESION100.)
 ECART-TYPE       .15   .48   .67   .20   .17  1.57    28.         6.  6.

*********************************************************************
* PROGRAMME TENSOR, VERSION R4DS 5  REFERENCE  8  J.ANGELIER,1975,1984 *
* SITE THRUST     TYPES CPS  POND.1  CHRONOL.9****  NBR=  5  TOT=  5.0 *
*********************************************************************

                     AXE SIGMA 1      D= 230.      P=  25.
                     AXE SIGMA 2      D= 139.      P=   0.
                     AXE SIGMA 3      D=  48.      P=  65.
                     RAPPORT PHI=  .181  PSI= -.770 RAD.

 MESURE  POIDS  SIGMA SIGMAN  TAU   RO  UPSILO  RMU   SIG,N     STR,T  45
    2.     1.0   1.74 -1.74   .02   .00   .85   .01     1. ??      1.
    8.     1.0   1.47  -.51  1.38   .31   .57  2.69    70.        13.
    9.     1.0   1.77  -.80  1.57   .51   .80  1.96    63.        19.
   10.     1.0   1.77  -.80  1.57   .16   .72  1.96    63.         6.
   11.     1.0   1.93  -.38  1.89   .46  1.07  5.04    79.        14.

 MESURE  POIDS  SIGMA SIGMAN  TAU   RO  UPSILO  RMU   SIG,N     STR,T  45
 MOYENNE   1.0   1.73  -.85  1.29   .29   .80  2.33    55.        11. 11.
 (COHESION100.)
 ECART-TYPE       .15   .48   .66   .19   .17  1.62    28.         6.  6.
```